Hindawi
Journal of Mathematics
Volume 2022, Article ID 9129187, 26 pages
https://doi.org/10.1155/2022/9129187

Research Article

Global Dynamics of a Within-Host COVID-19/AIDS Coinfection Model with Distributed Delays

S. A. Azoz,[1] **A. M. Elaiw**,[2,3] **E. Ramadan**,[1] **A. D. Al Agha**,[4] **and Aeshah A. Raezah**[5]

[1]*Department of Mathematics, Faculty of Science, Assiut University, Assiut, Egypt*
[2]*Department of Mathematics, Faculty of Science, King Abdulaziz University, P.O. Box 80203, Jeddah 21589, Saudi Arabia*
[3]*Department of Mathematics, Faculty of Science, Al-Azhar University, Assiut Branch, Assiut, Egypt*
[4]*Department of Mathematical Science, College of Engineering, University of Business and Technology, Jeddah 21361, Saudi Arabia*
[5]*Department of Mathematics, Faculty of Science, King Khalid University, Abha 62529, Saudi Arabia*

Correspondence should be addressed to S. A. Azoz; shaimaa.azoz@gmail.com

Received 11 July 2022; Revised 7 November 2022; Accepted 22 November 2022; Published 22 December 2022

Academic Editor: Chang Phang

Acquired immunodeficiency syndrome (AIDS) is a spectrum of conditions caused by infection with the human immunodeficiency virus (HIV). Among people with AIDS, cases of COVID-19 have been reported in many countries. COVID-19 (coronavirus disease 2019) is caused by the severe acute respiratory syndrome coronavirus 2 (SARS-CoV-2). In this manuscript, we are going to present a within-host COVID-19/AIDS coinfection model to study the dynamics and influence of the coinfection between COVID-19 and AIDS. The model is a six-dimensional delay differential equation that describes the interaction between uninfected epithelial cells, infected epithelial cells, free SARS-CoV-2 particles, uninfected $CD4^+$ T cells, infected $CD4^+$ T cells, and free HIV-1 particles. We demonstrated that the proposed model is biologically acceptable by proving the positivity and boundedness of the model solutions. The global stability analysis of the model is carried out in terms of the basic reproduction number. Numerical simulations are carried out to investigate that if COVID-19/AIDS coinfected individuals have a poor immune response or a low number of $CD4^+$ T cells, then the viral load of SARS-CoV-2 and the number of infected epithelial cells will rise. On the contrary, the existence of time delays can rise the number of uninfected $CD4^+$ T cells and uninfected epithelial cells, thus reducing the viral load within the host.

1. Introduction

In December 2019, the first case of the emergence of the severe acute respiratory syndrome coronavirus 2 (COVID-19) occurred in Wuhan, China. In March 2020, the World Health Organization (WHO) declared COVID-19 a worldwide epidemic. Globally, as of 27 April 2022, over 500 million people were infected with COVID-19, including 6 million deaths [1]. Old age and its accompanying symptoms such as diabetes, heart disease, and high blood pressure are considered risk factors for developing severe COVID-19 infection and are associated with a high death rate [2, 3]. Some other risk factors are associated when infection with COVID-19 occurs in people with chronic diseases such as acquired immunodeficiency syndrome (AIDS) [4]. In 2020, there were 37.7 million persons living with HIV-1 (PLWH) worldwide; HIV-1 causes acquired immunodeficiency syndrome (AIDS) with 680,000 of them dying from HIV-1-related diseases, and only 73% of them were on antiretroviral medication (ART) [5]. Because their immune systems are impaired, PLWH who do not receive ART or whose condition is poorly managed could be more susceptible to developing COVID-19. If infected with COVID-19, such people are at a greater risk of developing acute symptoms and dying. The coinfection cases are challenging due to the scarcity of data on the outcomes and consequences of SARS-CoV-2 infection in HIV-1 positive individuals [3, 6, 7].

HIV-1 and SARS-CoV-2 are both RNA viruses. SARS-CoV-2 attacks upper respiratory epithelial cells, and the

virus generated by infected cells goes down to the lower airway, infecting bronchial and alveolar epithelial cells [4, 8]. On the other hand, HIV-1 targets $CD4^+$ lymphocytes, which are the immune system's most plentiful white blood cells (referred to as $CD4^+$ T cells). A great effort is being made in many areas of the world to create measures to battle these viruses and study their biological and immunological features and clinical outcomes. Some of these studies indicate that COVID-19 pandemic has caused disruptions in HIV-1 care facilities in many countries [9, 10]. However, it is unclear whether people infected with HIV-1 having an increased incidence of COVID-19 and significant clinical signs, despite a controversial suggestion that antiretroviral therapy or HIV-1-related immunosuppression could protect HIV-1 infected people from severe COVID-19. A number of HIV-1 and SARS-CoV-2 coinfection cases have been documented throughout the world [11, 12]. Most studies of COVID-19/AIDS coinfection reported that there is a lack of clarity on what constitutes the primary illness and what constitutes comorbidity in the context of coinfection. Few studies inferred that SARS-CoV-2 infection does not increase the course of HIV-1 infection in PLWH nor does HIV-1 infection have an impact on COVID-19 infection course in PLWH [13–15]. However, Wang et al. [16] published a case report of an HIV-1/COVID-19 patient with such a lower $CD4^+$ T cell number, and as a result, the patient had a prolonged COVID-19 course and decreased antibody levels. Moreover, COVID-19/AIDS coinfection has been observed to cause pneumonia problems more frequently than COVID-19 alone [17]. This study aims to give a comprehensive picture of SARS-CoV-2 infection in persons having HIV-1/AIDS.

Mathematical models that consist of a system of differential equations have proven their effectiveness in studying the interactions between viruses and their hosts and the common interactions between diseases (see e.g., [12, 18–24]). HIV within-host models have been widely investigated and great results have been reached [18, 19, 25–28]. On the other side, SARS-CoV-2 within-host modeling has received less attention ([24, 29–32]). Some coinfection models between SARS-CoV-2 and other viruses have been developed. For example, Pinky and Dobrovolny [33] used a within-host model to investigate SARS-CoV-2 coinfections with several viruses types such as influenza A virus (IAV), parainfluenza virus (PIV), and human rhinovirus (HRV). In fact, the models of coinfection are essential to grasp the coinfection dynamics between SARS-CoV-2 and HIV, to assist the experimental studies and save time, and to develop effective treatments for coinfected people. Ahmed et al. [34] created a fractional epidemiological model to analyze the pandemic scenario in numerous HIV and COVID-19 affected countries, including South Africa and Brazil. Then, to the best of our knowledge, the first ordinary differential within-host SARS-CoV-2/HIV coinfection system is presented by Al Agha et al. [20]. The formulation of their model is based on Nowak and Bangham's model that was used widely to model HIV monoinfection and SARS-CoV-2 monoinfection. Al Agha et al. used the same principals to model SARS-CoV-2/HIV coinfection and connect the two infections together. The model is formulated as follows:

$$\begin{cases} \dot{X}(t) = \rho - \alpha X(t) - \eta X(t)V(t), \\ \dot{Y}(t) = \eta X(t)V(t) - kY(t) - \mu Y(t)S(t), \\ \dot{V}(t) = aY(t) - \delta V(t), \\ \dot{S}(t) = \xi + uY(t)S(t) - \gamma S(t) - \theta S(t)H(t), \\ \dot{W}(t) = \theta S(t)H(t) - \beta W(t), \\ \dot{H}(t) = \lambda W(t) - \omega H(t), \end{cases} \tag{1}$$

where $X(t)$, $Y(t)$, and $V(t)$ represent the healthy epithelial cells, infected epithelial cells, and free SARS-CoV-2 particles, respectively, whilst $S(t)$, $W(t)$, and $H(t)$ depict healthy $CD4^+$ T cells, infected $CD4^+$ T cells, and free HIV particles concentrations at time t, respectively. Epithelial cells are recruited at rate ρ and turned into infected cells at pace $\eta X(t)V(t)$. Infected produce SARS-CoV-2 particles at rate $aY(t)$. $CD4^+$ T cells are recruited at rate ξ, eliminate infected epithelial cells at a proportion $\mu Y(t)S(t)$, and proliferate at rate $uY(t)S(t)$. HIV particles infect $CD4^+$ T cells at rate $\theta S(t)H(t)$. The infected cells produces HIV at rate $\lambda W(t)$. The components $X(t)$, $Y(t)$, $Y(t)$, $Y(t)$, $W(t)$, and $H(t)$ die at rates $\alpha X(t)$, $kY(t)$, $\delta V(t)$, $\gamma S(t)$, $\beta W(t)$, and $\omega H(t)$, respectively. Then, Elaiw et al. [21] adopted the same previous model with the addition of the effect of latent cells, and then, they made a comprehensive study of the proposed model. Ringa et al. [22] presented a new mathematical model for COVID-19 and HIV/AIDS. The dynamics of the full model is driven by that of its submodels. Also, they studied the impact of intervention measures by incorporating it into the model using time-dependent controls.

Most of the previous publications are the assumptions that cells produce viruses immediately after they are infected. It is commonly observed that in many biological processes, a time delay is inevitable. For HIV-1 infection, it roughly takes about one day for a newly infected cell to become productive and then to be able to produce new virus particles. Therefore, mathematicians have frequently used different types of delays to make biological models more realistic. In [26, 28, 35], HIV models with time delay were introduced, whilst modeling and analysis of COVID-19 based on a time delay dynamic model are presented in [12, 23]. Although there are some publications that combine the coinfection between viruses in the presence of time delay, there are still no models of coinfection between SARS-CoV-2 and HIV with time delay. Due to the decisive role of time delays in dynamic systems, the objective of this work is to expand model (1) to accommodate distributed delays. This can help comprehend the coinfection dynamics between SARS-CoV-2 and HIV-1 from a different perspective. A continuous distribution function is used to represent the delay in case of distributed time delay. This makes distributed delays more realistic than discrete time delays which presume that each individual in the population has the same delay period. Thus, we have investigated a model with six delay differential equations, and we have established the solutions nonnegativity and boundedness, listed the

prospective equilibrium points and the conditions of existence, discussed the global stability of the equilibria, and examined time delay impact on the model's dynamics. The document includes the following sections: the model is presented in Section 2. Section 3 confirms the basic properties of the model. Section 4 exhibits the global properties of the model. Section 5 lists the numerical simulations. Finally, Section 6 debates the results and some potential next directions.

2. COVID-19/AIDS Coinfection Model with Distributed Delay

In this section, we extend model (1) by considering a variety of distributed time delays as follows:

$$\begin{cases} \dot{X}(t) = \rho - \alpha X(t) - \eta X(t)V(t), \\ \dot{Y}(t) = \eta \int_0^\infty g_1(\epsilon) e^{-m_1\epsilon} X(t-\epsilon)V(t-\epsilon)\mathrm{d}\epsilon - kY(t) - \upsilon Y(t)S(t), \\ \dot{V}(t) = a \int_0^\infty g_2(\epsilon) e^{-m_2\epsilon} Y(t-\epsilon)\mathrm{d}\epsilon - \wp V(t), \\ \dot{S}(t) = \xi + \iota Y(t)S(t) - \gamma S(t) - \mathfrak{F} S(t)H(t), \\ \dot{W}(t) = \mathfrak{F} \int_0^\infty g_3(\epsilon) e^{-m_3\epsilon} S(t-\epsilon)H(t-\epsilon)\mathrm{d}\epsilon - \beta W(t), \\ \dot{H}(t) = \lambda \int_0^\infty g_4(\epsilon) e^{-m_4\epsilon} W(t-\epsilon)\mathrm{d}\epsilon - \omega H(t). \end{cases} \tag{2}$$

Thus, we have a system of six delay differential equations where $X(t)$, $Y(t)$, $V(t)$, $S(t)$, $W(t)$, and $H(t)$ stand for the concentrations of uninfected epithelial cells, infected epithelial cells, free SARS-CoV-2 particles, uninfected $CD4^+$ T cells, infected $CD4^+$ T cells, and HIV-1 particles at time t, respectively. A scheme describing the coinfection between SARS-CoV-2 and HIV in host without time delay is shown in Figure 1. The factor $g_1(\varepsilon)e^{-m_1\varepsilon}$ designates the likelihood that uninfected epithelial cells were in touch with SARS-CoV-2 particles at time $t-\epsilon$ survived ϵ time units, and infection occurs at time t. The term $g_2(\epsilon)e^{-m_2\epsilon}$ simulates the probability of new immature SARS-CoV-2 particles at time $t-\epsilon$ survived ϵ time units and mature at time t. Moreover, the factor $g_3(\epsilon)e^{-m_3\epsilon}$ symbolizes the probability that uninfected $CD4^+$ T cells contacted by HIV-1 particles at time $t-\epsilon$ survived ϵ time units and become infected at time t. The term $g_4(\epsilon)e^{-m_4\epsilon}$ represents the probability that new immature HIV-1 particles at time $t-\epsilon$ persisted ϵ time units and mature at time t, where m_i and $i = 1, 2, 3, 4$, and are the positive constants. The delay parameter ϵ is a random variable picked from probability distribution functions $g_i(\epsilon)$ during time interval $[0, \infty)$. The functions $g_i(\epsilon)$ $(i = 1, 2, 3, 4)$ satisfy $g_i(\epsilon) > 0$ and

$$\begin{aligned} \int_0^\infty g_i(\epsilon)\mathrm{d}\epsilon &= 1, \\ \int_0^\infty g_i(\epsilon)e^{-n\epsilon}\mathrm{d}\epsilon &< \infty, \end{aligned} \tag{3}$$

where $n > 0$. Let us denote the following model:

$$\begin{aligned} \overline{\mathscr{L}}_i(\epsilon) &= g_i(\epsilon)e^{-m_i\epsilon}, \\ L_i &= \int_0^\infty \overline{\mathscr{L}}_i(\epsilon)\mathrm{d}\epsilon, \end{aligned} \tag{4}$$

where $i = 1, 2, 3, 4$. This implies that $0 < L_i \le 1$. The initial conditions of model (2) are specified as follows:

$$\begin{cases} X(\varpi) = \varphi_1(\varpi), \quad Y(\varpi) = \varphi_2(\varpi), \quad V(\varpi) = \varphi_3(\varpi), \\ S(\varpi) = \varphi_4(\varpi), \quad W(\varpi) = \varphi_5(\varpi), \quad H(\varpi) = \varphi_6(\varpi), \\ \varphi_j(\varpi) \ge 0, \quad \varpi \in (-\infty, 0], \quad j = 1, 2, \ldots 6, \end{cases} \tag{5}$$

where $\varphi_j(\varpi) \in \mathbb{C} = \{\zeta \in C([-\infty, 0), \mathbb{R})\colon \zeta(\theta)e^{\alpha\theta}$ is uniformly *continuous* for *continuous for* $\theta \in [-\infty, 0), \|\zeta\| < \infty\}$, and $\|\zeta\| = \sup_{\theta\le 0}|\zeta(\theta)|e^{\alpha\theta}$ such that α is a positive constant. Here, $\mathbb{C}$ is the Banach space of fading memory type [36]. Therefore, using the standard theory of differential equations with infinitely distributed delays [37, 38], model (2) with initial constraints (3) has a single solution.

3. Basic Characteristics

This section proves that model (2) solutions are non-negative and ultimately bounded. Additionally, it computes whole potential equilibria and the threshold numbers.

3.1. Non-Negativity and Boundedness

Proposition 1. *All of model (2) solutions with beginning conditions (3) are non-negative and eventually bounded.*

Proof. Starting with model (2) first equation, we obtain $\dot{X}(t)|_{X=0} = \rho > 0$, which yields that $X(t) > 0$ for all $t \ge 0$. From fourth equation of the model, we get $\dot{S}(t)|_{S=0} = \xi > 0$; then, $S(t) > 0$ for all $t \ge 0$. Furthermore, the rest of the model equations give us the following model:

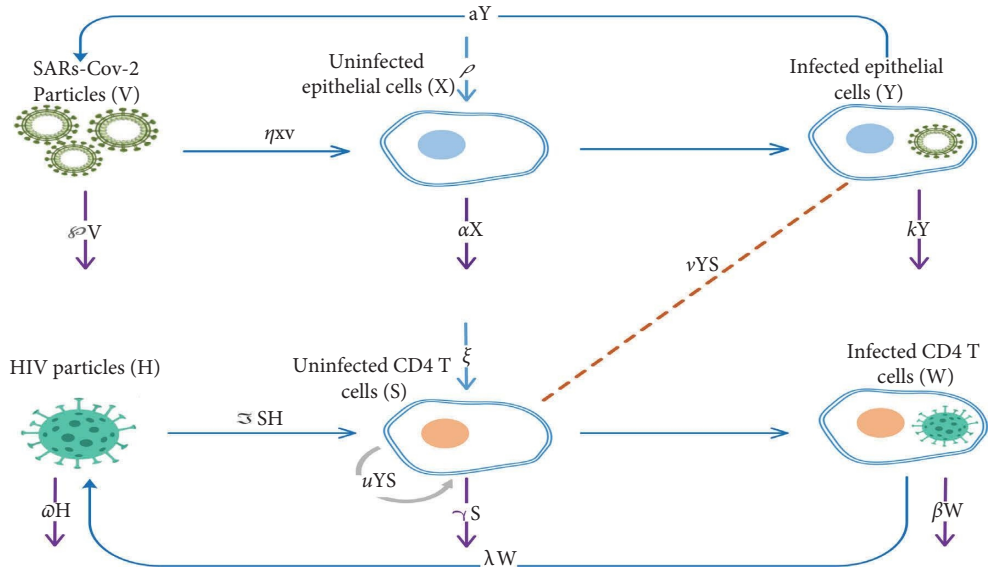

Figure 1: Scheme describing the coinfection between SARS-CoV-2 and HIV.

$$
\begin{aligned}
Y(t) &= \varphi_2(0)e^{-\int_0^t (k+vs(q))\mathrm{d}q} + \eta\int_0^t e^{-\int_\ell^t (k+vs(q))\mathrm{d}q}\int_0^\infty \overline{\mathscr{L}}_1(\epsilon)X(\ell-\epsilon)V(\ell-\epsilon)\mathrm{d}\epsilon\mathrm{d}\ell \geq 0,\\
V(t) &= \varphi_3(0)e^{-\wp t} + a\int_0^t e^{-\wp(t-\ell)}\int_0^\infty \overline{\mathscr{L}}_2(\epsilon)Y(\ell-\epsilon)\mathrm{d}\epsilon\mathrm{d}\ell \geq 0,\\
W(t) &= \varphi_5(0)e^{-\beta t} + \Im\int_0^t e^{-\beta(t-\ell)}\int_0^\infty \overline{\mathscr{L}}_3(\epsilon)S(\ell-\epsilon)H(\ell-\epsilon)\mathrm{d}\epsilon\mathrm{d}\ell \geq 0,\\
H(t) &= \varphi_6(0)e^{-\omega t} + \lambda\int_0^t e^{-\omega(t-\ell)}\int_0^\infty \overline{\mathscr{L}}_4(\epsilon)W(\ell-\epsilon)\mathrm{d}\epsilon\mathrm{d}\ell \geq 0.
\end{aligned}
\tag{6}
$$

For all $t \in [0,\infty)$, as a result of the recursive argument, we obtain $X(t), Y(t), V(t), S(t), W(t), H(t) \geq 0$ for all $t \geq 0$. Hence, system (2) solutions with initial conditions (3) realize $(X(t), Y(t), V(t), S(t), W(t), H(t)) \in \mathbb{R}^6_{\geq 0}$ for all nonnegative values of t.

Now, we establish the boundedness of the model's solutions. Based on model (2) first equation, we gain $\lim_{t\longrightarrow\infty}\sup X(t) \leq \Omega_1$, where $\Omega_1 = \rho/\alpha$. We define the following model:

$$
\Psi_1(t) = \int_0^\infty \overline{\mathscr{L}}_1(\varepsilon)X(t-\varepsilon)\mathrm{d}\varepsilon + Y(t) + \frac{v}{u}S(t). \tag{7}
$$

Then, we get the following model:

$$
\begin{aligned}
\dot{\Psi}_1(t) &= \int_0^\infty \overline{\mathscr{L}}_1(\varepsilon)[\rho - \alpha X(t-\varepsilon) - \eta X(t-\varepsilon)V(t-\varepsilon)]\mathrm{d}\varepsilon + \eta\int_0^\infty \overline{\mathscr{L}}_1(\varepsilon)X(t-\varepsilon)V(t-\varepsilon)\mathrm{d}\varepsilon\\
&\quad - kY(t) - vY(t)S(t) + \frac{v}{u}[\xi + uY(t)S(t) - \gamma S(t) - \Im S(t)H(t)]\\
&\leq \rho\int_0^\infty \overline{\mathscr{L}}_1(\varepsilon)\mathrm{d}\varepsilon + \frac{v\xi}{u} - \alpha\int_0^\infty \overline{\mathscr{L}}_1(\varepsilon)X(t-\varepsilon)\mathrm{d}\varepsilon - kY(t) - \frac{v\gamma}{u}S(t)\\
&\leq \rho + \frac{v\xi}{u} - \phi_1\left[\int_0^\infty \overline{\mathscr{L}}_1(\varepsilon)X(t-\varepsilon)\mathrm{d}\varepsilon + Y(t) + \frac{v}{u}S(t)\right]\\
&= \rho + \frac{v\xi}{u} - \phi_1\Psi_1(t),
\end{aligned}
\tag{8}
$$

where $\phi_1 = \min\{\alpha, k, \gamma\}$. This implies that $\lim_{t\longrightarrow\infty}\sup\Psi_1(t) \le \Omega_2$, where $\Omega_2 = \rho/\phi_1 + \upsilon\xi/u\phi_1$. Since $Y(t)$ and $S(t)$ are non-negative, then $\lim_{t\longrightarrow\infty}\sup Y(t) \le \Omega_2$ and $\lim_{t\longrightarrow\infty}\sup S(t) \le \Omega_3$, where $\Omega_3 = u\Omega_2/\upsilon$. Using model (2) third equation, we get the following model:

$$\dot{V}(t) = a\int_0^\infty \overline{\mathscr{L}}_2(\epsilon)Y(t-\epsilon)\mathrm{d}\epsilon - \wp V(t) \le aL_2\Omega_2 - \wp V(t) \le a\Omega_2 - \wp V(t). \tag{9}$$

This implies that $\lim_{t\longrightarrow\infty}\sup V(t) \le \Omega_4$, where $\Omega_4 = a\Omega_2/\wp$.

We define the following model:

$$\Psi_2(t) = \int_0^\infty \overline{\mathscr{L}}_3(\varepsilon)S(t-\varepsilon)\mathrm{d}\varepsilon + W(t). \tag{10}$$

Following that, we get the following model:

$$\begin{aligned}\dot{\Psi}_2(t) = &\int_0^\infty \overline{\mathscr{L}}_3(\varepsilon)[\xi + uY(t-\varepsilon)S(t-\varepsilon) - \gamma S(t-\varepsilon) - \mathfrak{T}S(t-\varepsilon)H(t-\varepsilon)]\mathrm{d}\varepsilon\\ &+ \mathfrak{T}\int_0^\infty \overline{\mathscr{L}}_3(\varepsilon)S(t-\varepsilon)H(t-\varepsilon)\mathrm{d}\varepsilon - \beta W(t) \le \xi + u\Omega_2\Omega_3 - \phi_2\Psi_2(t),\end{aligned} \tag{11}$$

where $\phi_2 = \min\{\gamma, \beta\}$. Thus, we have $\lim_{t\longrightarrow\infty}\sup W(t) \le \Omega_5$, where $\Omega_5 = (\xi + u\Omega_2\Omega_3)/\phi_2$. Finally, the last equation of model (2) gives the following model:

$$\dot{H}(t) = \lambda\int_0^\infty \overline{\mathscr{L}}_4(\epsilon)W(t-\epsilon)\mathrm{d}\epsilon - \omega H(t) \le \lambda\Omega_5 - \omega H(t). \tag{12}$$

Thus, $\lim_{t\longrightarrow\infty}\sup H(t) \le \Omega_6$, where $\Omega_6 = \lambda\Omega_5/\omega$. Accordingly, the following region is positively invariant with regard to model (2).

$$\Xi = \left\{(X, Y, V, S, W, H) \in C^6_{\ge 0}\colon \|X\| \le \Omega_1, \|Y\| \le \Omega_2, \|V\| \le \Omega_4, \|S\| \le \Omega_3, \|W\| \le \Omega_5, \|H\| \le \Omega_6\right\}. \tag{13}$$

□

3.2. Equilibrium Points. This subsection displays all of model (2) possible equilibrium states and deduces four threshold parameters that determine the equilibria existence.

We solve the following set of algebraic equations to calculate the following model equilibrium points:

$$\begin{cases} 0 = \rho - \alpha X - \eta XV,\\ 0 = \eta L_1 XV - kY - \upsilon YS,\\ 0 = aL_2 Y - \wp V,\\ 0 = \xi + uYS - \gamma S - \mathfrak{T}SH,\\ 0 = \mathfrak{T}L_3 SH - \beta W,\\ 0 = \lambda L_4 W - \omega H. \end{cases} \tag{14}$$

From last equation of model (4), we have $W = \omega H/\lambda L_4$. Then, we substitute in the fifth equation, and we get the following model:

$$0 = \left(\mathfrak{T}L_3 S - \frac{\beta\omega}{\lambda L_4}\right)H. \tag{15}$$

So, we have two possibilities:

$$H = 0 \text{ or } S = \frac{\beta\omega}{\lambda\mathfrak{T}L_3 L_4}. \tag{16}$$

Then, doing the same for second and third equations, we obtain another two possibilities as follows:

$$V = 0 \text{ or } \eta L_1 X - \frac{k\rho}{aL_2} - \frac{\upsilon\rho S}{aL_2} = 0. \tag{17}$$

Equations (16) and (17) provide us with four possibilities. Accordingly, model (4) has four equilibrium points:

(i) Uninfected equilibrium $EP_0 = (X_0, 0, 0, S_0, 0, 0)$, where $X_0 = \rho/\alpha$ and $S_0 = \xi/\gamma$

(ii) The HIV-1 monoinfection equilibrium $EP_H = (X_1, 0, 0, S_1, W_1, H_1)$, where

$$\begin{aligned} X_1 &= \frac{\rho}{\alpha},\ S_1 = \frac{\beta\omega}{\mathfrak{T}\lambda L_3 L_4},\\ W_1 &= \frac{\gamma\omega}{\mathfrak{T}\lambda L_4}\left(\frac{\xi\mathfrak{T}\lambda L_3 L_4}{\beta\gamma\omega} - 1\right),\\ H_1 &= \frac{\gamma}{\mathfrak{T}}\left(\frac{\xi\mathfrak{T}\lambda L_3 L_4}{\beta\gamma\omega} - 1\right). \end{aligned} \tag{18}$$

It follows that $W_1 > 0$ and $H_1 > 0$ only when $\xi\mathfrak{T}\lambda L_3 L_4/\beta\gamma\omega > 1$. Thus, we have the following model:

$$X_1 = X_0,\ S_1 = \frac{S_0}{R_1},$$
$$W_1 = \frac{\gamma\omega}{\mathfrak{J}\lambda L_4}(R_1 - 1), \tag{19}$$
$$H_1 = \frac{\gamma}{\mathfrak{J}}(R_1 - 1).$$

Here, $R_1 = \xi\mathfrak{J}\lambda L_3 L_4/\beta\gamma\omega$. Here, R_1 is the basic reproduction number for HIV-1 infection. It sets start of HIV-1 infection in host body. We note that $W_1 > 0$ and $H_1 > 0$ if $R_1 > 1$. Therefore, EP_H exists when $R_1 > 1$.

(iii) SARS-CoV-2 monoinfection equilibrium $EP_V = (X_2, Y_2, V_2, S_2, 0, 0)$, where

$$X_2 = \frac{Y_2 k + S_2 Y_2 \upsilon}{\eta V_2 L_1},$$
$$Y_2 = \frac{\wp V_2}{aL_2}, \tag{20}$$
$$S_2 = \frac{\xi}{\gamma - uY_2}.$$

V_2 satisfies the following equation:

$$\frac{u\wp^2\eta k V_2^2 + \left(ua\wp^2 k - a\gamma\wp\eta k L_2 - a\wp\eta\upsilon\xi L_2 - au\wp\eta\rho L_1 L_2\right)V_2 - aa\gamma\wp k L_2 - aa\wp\upsilon\xi L_2 + a^2\gamma\eta\rho L_1 L_2^2}{a\eta L_1 L_2(a\gamma L_2 - u\wp V_2)} = 0. \tag{21}$$

To prove that equation (21) has a positive root, we introduce a function $B(V)$ as follows:

$$B(V) = \frac{u\wp^2\eta k V^2 + \left(ua\wp^2 k - a\gamma\wp\eta k L_2 - a\wp\eta\upsilon\xi L_2 - au\wp\eta\rho L_1 L_2\right)V - aa\gamma\wp k L_2 - aa\wp\upsilon\xi L_2 + a^2\gamma\eta\rho L_1 L_2^2}{a\eta L_1 L_2(a\gamma L_2 - u\wp V)}. \tag{22}$$

Then, we have the following equation:

$$B(0) = \frac{-aa\gamma\wp k L_2 - aa\wp\upsilon\xi L_2 + a^2\gamma\eta\rho L_1 L_2^2}{a^2\gamma\eta L_1 L_2^2} = \frac{\alpha\gamma\wp k + \alpha\wp\upsilon\xi}{a\gamma\eta L_1 L_2}(R_2 - 1). \tag{23}$$

Here, $R_2 = a\gamma\eta\rho L_1 L_2/\alpha\wp(\gamma k + \upsilon\xi)$. This implies that $B(0) > 0$ when $R_2 > 1$. In addition, we find that

$$\lim_{V \longrightarrow \frac{a\gamma L_2}{u\wp}^-} B(V) = -\infty. \tag{24}$$

It follows that there exists $0 < V_2 < a\gamma L_2/u\wp$ such that $B(V_2) = 0$. From equation (20), we get $Y_2 > 0$, $S_2 > 0$, and $X_2 > 0$. As a result, we deduce that EP_V exists when $R_2 > 1$. Here, R_2 is the basic reproduction number for SARS-CoV-2 infection. It defines start of SARS-CoV-2 infection in host body.

(iv) COVID-19/AIDS coinfection equilibrium $EP_{VH} = (X_3, Y_3, V_3, S_3, W_3, H_3)$, where

$$X_3 = \frac{\wp(k\mathfrak{J}\lambda L_3 L_4 + \beta\upsilon\omega)}{a\eta\mathfrak{J}\lambda L_1 L_2 L_3 L_4}, Y_3 = \frac{\alpha\wp}{a\eta L_2}\left(\frac{a\eta\mathfrak{J}\lambda\rho L_1 L_2 L_3 L_4}{\alpha\wp(\mathfrak{J}k\lambda L_3 L_4 + \beta\upsilon\omega)} - 1\right),$$
$$V_3 = \frac{\alpha}{\eta}\left(\frac{a\eta\mathfrak{J}\lambda\rho L_1 L_2 L_3 L_4}{\alpha\wp(\mathfrak{J}k\lambda L_3 L_4 + \beta\upsilon\omega)} - 1\right), S_3 = \frac{\beta\omega}{\mathfrak{J}\lambda L_3 L_4},$$
$$W_3 = \frac{\omega(ua\wp + a\gamma\eta L_2)}{a\eta\mathfrak{J}\lambda L_2 L_4}\left[\left(\frac{\lambda\xi}{\beta\omega} + \frac{u\lambda\rho L_1}{\mathfrak{J}k\lambda L_3 L_4 + \beta\upsilon\omega}\right)\frac{a\eta\mathfrak{J}L_2 L_3 L_4}{ua\wp + a\gamma\eta L_2} - 1\right], \tag{25}$$
$$H_3 = \frac{ua\wp + a\gamma\eta L_2}{a\eta\mathfrak{J}L_2}\left[\left(\frac{\lambda\xi}{\beta\omega} + \frac{u\lambda\rho L_1}{\mathfrak{J}k\lambda L_3 L_4 + \beta\upsilon\omega}\right)\frac{a\eta\mathfrak{J}L_2 L_3 L_4}{ua\wp + a\gamma\eta L_2} - 1\right].$$

It follows that $W_3 > 0$ and $H_3 > 0$ only when $(\lambda\xi/\beta\omega + u\lambda\rho L_1/\mathfrak{F}k\lambda L_3L_4 + \beta\upsilon\omega)a\eta\mathfrak{F}L_2L_3L_4/u\alpha\wp + a\gamma\eta L_2 > 1$. On the other hand, $Y_3 > 0$ and $V_3 > 0$ only when $a\eta\mathfrak{F}\lambda\rho L_1L_2L_3L_4/\alpha\wp(\mathfrak{F}k\lambda L_3L_4 + \beta\upsilon\omega) > 1$.

Thus, we can rewrite the components of EP_{VH} as follows:

$$\begin{aligned} X_3 &= \frac{X_0}{R_4}, \\ Y_3 &= \frac{\alpha\wp}{a\eta L_2}(R_4 - 1), \\ V_3 &= \frac{\alpha}{\eta}(R_4 - 1), \\ S_3 &= \frac{\beta\omega}{\mathfrak{F}\lambda L_3L_4}, \\ W_3 &= \frac{\omega(u\alpha\wp + a\gamma\eta L_2)}{a\eta\mathfrak{F}\lambda L_2L_4}(R_3 - 1), \\ H_3 &= \frac{u\alpha\wp + a\gamma\eta L_2}{a\eta\mathfrak{F}L_2}(R_3 - 1), \end{aligned} \tag{26}$$

where

$$\begin{aligned} R_3 &= \left(\frac{\lambda\xi}{\beta\omega} + \frac{u\lambda\rho L_1}{\mathfrak{F}k\lambda L_3L_4 + \beta\upsilon\omega}\right)\frac{a\eta\mathfrak{F}L_2L_3L_4}{u\alpha\wp + a\gamma\eta L_2}, \\ R_4 &= \frac{a\eta\mathfrak{F}\lambda\rho L_1L_2L_3L_4}{\alpha\wp(\mathfrak{F}k\lambda L_3L_4 + \beta\upsilon\omega)}. \end{aligned} \tag{27}$$

Therefore, EP_{VH} exists when $R_3 > 1$ and $R_4 > 1$. Here, R_3 and R_4 are the threshold parameters that mark the COVID-19/AIDS coinfection incidence.

The threshold parameters are defined as follows:

$$\begin{cases} R_1 = \dfrac{\xi\mathfrak{F}\lambda L_3L_4}{\beta\gamma\omega}, \\ R_2 = \dfrac{a\gamma\eta\rho L_1L_2}{\alpha\wp(\gamma k + \upsilon\xi)}, \\ R_3 = \left(\dfrac{\lambda\xi}{\beta\omega} + \dfrac{u\lambda\rho L_1}{\mathfrak{F}k\lambda L_3L_4 + \beta\upsilon\omega}\right)\dfrac{a\eta\mathfrak{F}L_2L_3L_4}{u\alpha\wp + a\gamma\eta L_2}, \\ R_4 = \dfrac{a\eta\mathfrak{F}\lambda\rho L_1L_2L_3L_4}{\alpha\wp(\mathfrak{F}k\lambda L_3L_4 + \beta\upsilon\omega)}. \end{cases} \tag{28}$$

For simplicity, the contractions listed will be used in the parts that follow

$$\begin{aligned} X(t) \equiv X, Y(t) \equiv Y, V(t) \equiv V, \\ S(t) \equiv S, W(t) \equiv W, H(t) \equiv H, \end{aligned} \tag{29}$$

and

$$\begin{aligned} X(t-\epsilon) \equiv X_\epsilon, Y(t-\epsilon) \equiv Y_\epsilon, V(t-\epsilon) \equiv V_\epsilon, \\ S(t-\epsilon) \equiv S_\epsilon, W(t-\epsilon) \equiv W_\epsilon, H(t-\epsilon) \equiv H_\epsilon. \end{aligned} \tag{30}$$

4. Global Properties

We demonstrate the global asymptotic stability of all equilibria in this section by building Lyapunov functions using the approach described in [39]. We define $F(\Delta) = \Delta - 1 - \ln\Delta$, where Δ can be any variable for the model.

Theorem 1. *Globally asymptotically stable (G.A.S) of equilibrium EP_0 is satisfied when $R_1 \le 1$ and $R_2 \le 1$.*

Proof. Take a Lyapunov function $\vartheta_0(X, Y, V, S, W, H)$ as follows:

$$\begin{aligned} \vartheta_0 = {} & X_0F\left(\frac{X}{X_0}\right) + \frac{1}{L_1}Y + \frac{\eta X_0}{\wp}V + \frac{\upsilon}{uL_1}S_0F\left(\frac{S}{S_0}\right) + \frac{\upsilon}{uL_1L_3}W + \frac{\upsilon\beta}{u\lambda L_1L_3L_4}H \\ & + \frac{\eta}{L_1}\int_0^\infty \overline{\mathscr{L}}_1(\varepsilon)\int_{t-\varepsilon}^t X(\ell)V(\ell)\mathrm{d}\ell\mathrm{d}\varepsilon + \frac{a\eta X_0}{\wp}\int_0^\infty \overline{\mathscr{L}}_2(\varepsilon)\int_{t-\varepsilon}^t Y(\ell)\mathrm{d}\ell\mathrm{d}\varepsilon \\ & + \frac{\upsilon\mathfrak{F}}{uL_1L_3}\int_0^\infty \overline{\mathscr{L}}_3(\varepsilon)\int_{t-\varepsilon}^t S(\ell)H(\ell)\mathrm{d}\ell\mathrm{d}\varepsilon + \frac{\upsilon\beta}{uL_1L_3L_4}\int_0^\infty \overline{\mathscr{L}}_4(\ell)\int_{t-\varepsilon}^t W(\ell)\mathrm{d}\ell\mathrm{d}\varepsilon. \end{aligned} \tag{31}$$

Clearly, $\vartheta_0(X,Y,V,S,W,H) > 0$ for all $X,Y,V,S,W,H > 0$ and $\vartheta_0(X_0,0,0,S_0,0,0) = 0$. Calculating $\mathrm{d}\vartheta_0/\mathrm{d}t$ along the solutions of system (2) gives the following equation:

$$\begin{aligned}\frac{\mathrm{d}\vartheta_0}{\mathrm{d}t} &= \left(1-\frac{X_0}{X}\right)[\rho-\alpha X-\eta XV]+\frac{1}{L_1}\left[\eta\int_0^\infty \overline{\mathscr{Z}}_1(\varepsilon)X_\varepsilon V_\varepsilon \mathrm{d}\varepsilon - kY - \upsilon YS\right]+\frac{\eta X_0}{\wp}\left[a\int_0^\infty \overline{\mathscr{Z}}_2(\varepsilon)Y_\varepsilon \mathrm{d}\varepsilon - \wp V\right]\\ &+\frac{\upsilon}{uL_1}\left(1-\frac{S_0}{S}\right)[\xi+uYS-\gamma S-\mathfrak{T}SH]+\frac{\upsilon}{uL_1L_3}\left[\mathfrak{T}\int_0^\infty \overline{\mathscr{Z}}_3(\varepsilon)S_\varepsilon H_\varepsilon \mathrm{d}\varepsilon - \beta W\right]\\ &+\frac{\upsilon\beta}{u\lambda L_1L_3L_4}\left[\lambda\int_0^\infty \overline{\mathscr{Z}}_4(\varepsilon)W_\varepsilon \mathrm{d}\varepsilon - \omega H\right]+\frac{\eta}{L_1}\int_0^\infty \overline{\mathscr{Z}}_1(\varepsilon)[XV-X_\varepsilon V_\varepsilon]\mathrm{d}\varepsilon+\frac{a\eta X_0}{\wp}\int_0^\infty \overline{\mathscr{Z}}_2(\varepsilon)[Y-Y_\varepsilon]\mathrm{d}\varepsilon\\ &+\frac{\upsilon\mathfrak{T}}{uL_1L_3}\int_0^\infty \overline{\mathscr{Z}}_3(\varepsilon)[SH-S_\varepsilon H_\varepsilon]d\varepsilon+\frac{\upsilon\beta}{uL_1L_3L_4}\int_0^\infty \overline{\mathscr{Z}}_4(\varepsilon)[W-W_\varepsilon]\mathrm{d}\varepsilon.\end{aligned} \tag{32}$$

Adding up the terms in equation (32), we obtain the following equation:

$$\begin{aligned}\frac{d\vartheta_0}{dt} &= \left(1-\frac{X_0}{X}\right)(\rho-\alpha X)-\eta XV+\eta X_0V-\frac{1}{L_1}kY-\frac{1}{L_1}\upsilon YS-\eta X_0V+\frac{\upsilon}{uL_1}\left(1-\frac{S_0}{S}\right)(\xi-\gamma S)\\ &+\frac{1}{L_1}\upsilon YS-\frac{1}{L_1}\upsilon YS_0-\frac{\upsilon}{uL_1}\mathfrak{T}SH+\frac{\upsilon}{uL_1}\mathfrak{T}S_0H-\frac{\upsilon\beta}{uL_1L_3}W-\frac{\upsilon\beta\omega}{u\lambda L_1L_3L_4}H+\eta XV+\frac{a\eta X_0}{\wp}L_2Y\\ &+\frac{\upsilon}{uL_1}\mathfrak{T}SH+\frac{\upsilon\beta}{uL_1L_3}W.\end{aligned} \tag{33}$$

Using $\rho = \alpha X_0$ and $\xi = \gamma S_0$, we obtain the following equation:

$$\begin{aligned}\frac{\mathrm{d}\vartheta_0}{\mathrm{d}t} &= -\frac{\alpha}{X}(X-X_0)^2-\frac{\upsilon\gamma}{uL_1S}(S-S_0)^2+\left(\frac{\eta X_0}{\wp}aL_2-\frac{1}{L_1}k-\frac{1}{L_1}\upsilon S_0\right)Y+\frac{\upsilon}{uL_1}\left(\mathfrak{T}S_0-\frac{\beta\omega}{\lambda L_3L_4}\right)H\\ &= -\frac{\alpha}{X}(X-X_0)^2-\frac{\upsilon\gamma}{uL_1S}(S-S_0)^2+\frac{\gamma k+\upsilon\xi}{\gamma L_1}\left(\frac{a\gamma\eta\rho L_1L_2}{\alpha\wp(\gamma k+\upsilon\xi)}-1\right)Y+\frac{\upsilon\beta\omega}{u\lambda L_1L_3L_4}\left(\frac{\xi\mathfrak{T}\lambda L_3L_4}{\beta\gamma\omega}-1\right)H\\ &= -\frac{\alpha}{X}(X-X_0)^2-\frac{\upsilon\gamma}{uL_1S}(S-S_0)^2+\frac{\gamma k+\upsilon\xi}{\gamma L_1}(R_2-1)Y+\frac{\upsilon\beta\omega}{u\lambda L_1L_3L_4}(R_1-1)H.\end{aligned} \tag{34}$$

Since $R_1 \le 1$ and $R_2 \le 1$, we get $\mathrm{d}\vartheta_0/\mathrm{d}t \le 0$ for all $X,Y,V,S,W,H > 0$. Also, $\mathrm{d}\vartheta_0/\mathrm{d}t = 0$ when $X = X_0$, $S = S_0$, and $Y = H = 0$. Set $T_0 = \{(X,Y,V,S,W,H)\colon \mathrm{d}\vartheta_0/\mathrm{d}t = 0\}$ and the largest invariant subset (L.I.S) of T_0 by T_0'. Then, the model solutions converge to T_0'. The set T_0' contains elements with $X(t) = X_0$, $S(t) = S_0$, and $Y(t) = H(t) = 0$, and hence, $\dot{Y}(t) = \dot{H}(t) = 0$. The second and last equations of the model (2) give the following equation:

$$0 = \dot{Y}(t) = \eta \int_0^{\infty} \overline{\mathscr{F}}_1(\epsilon) X_0 V_{\epsilon} \mathrm{d}\epsilon,$$
$$0 = \dot{H}(t) = \lambda \int_0^{\infty} \overline{\mathscr{F}}_4(\epsilon) W_{\epsilon} \mathrm{d}\epsilon. \tag{35}$$

Thus, we get $V(t) = W(t) = 0$ for all t. Then, $T_0' = \{EP_0\}$, and using Lyapunov–LaSalle asymptotic stability theorem [40–42], EP_0 is G.A.S. □

In the following theorems, we need to use the equalities:

$$\begin{cases} \ln\left(\frac{S_{\varepsilon}H_{\varepsilon}}{SH}\right) = \ln\left(\frac{S_{\varepsilon}H_{\varepsilon}W_j}{S_jH_jW}\right) + \ln\left(\frac{S_j}{S}\right) + \ln\left(\frac{WH_j}{W_jH}\right), \\ \ln\left(\frac{W_{\varepsilon}}{W}\right) = \ln\left(\frac{W_{\varepsilon}H_j}{W_jH}\right) + \ln\left(\frac{W_jH}{WH_j}\right), \quad j = 1, 3. \end{cases} \tag{36}$$

Furthermore,

$$\begin{cases} \ln\left(\frac{X_{\epsilon}V_{\epsilon}}{XV}\right) = \ln\left(\frac{X_{\epsilon}V_{\epsilon}Y_i}{X_iV_iY}\right) + \ln\left(\frac{X_i}{X}\right) + \ln\left(\frac{YV_i}{Y_iV}\right), \\ \ln\left(\frac{Y_{\epsilon}}{Y}\right) = \ln\left(\frac{Y_{\epsilon}V_i}{Y_iV}\right) + \ln\left(\frac{Y_iV}{YV_i}\right), \quad i = 2, 3. \end{cases} \tag{37}$$

Theorem 2. *If $R_1 > 1$ and $R_4 \le 1$, the equilibrium EP_H is G.A.S.*

Proof. Consider a Lyapunov function $\vartheta_1(X, Y, V, S, W, H)$ as follows:

$$\begin{aligned} \vartheta_1 = {} & X_1 F\left(\frac{X}{X_1}\right) + \frac{1}{L_1} Y + \frac{\eta X_1}{\wp} V + \frac{v}{uL_1} S_1 F\left(\frac{S}{S_1}\right) + \frac{v}{uL_1L_3} W_1 F\left(\frac{W}{W_1}\right) + \frac{v\beta}{u\lambda L_1L_3L_4} H_1 F\left(\frac{H}{H_1}\right) \\ & + \frac{\eta}{L_1} \int_0^{\infty} \overline{\mathscr{F}}_1(\varepsilon) \int_{t-\varepsilon}^{t} X(\ell) V(\ell) \mathrm{d}\ell \mathrm{d}\varepsilon + \frac{a\eta X_1}{\wp} \int_0^{\infty} \overline{\mathscr{F}}_2(\varepsilon) \int_{t-\varepsilon}^{t} Y(l) \mathrm{d}\ell \mathrm{d}\varepsilon \\ & + \frac{v\mathfrak{F}S_1H_1}{uL_1L_3} \int_0^{\infty} \overline{\mathscr{F}}_3(\varepsilon) \int_{t-\varepsilon}^{t} F\left(\frac{S(\ell)H(\ell)}{S_1H_1}\right) \mathrm{d}\ell \mathrm{d}\varepsilon + \frac{v\beta W_1}{uL_1L_3L_4} \int_0^{\infty} \overline{\mathscr{F}}_4(\varepsilon) \int_{t-\varepsilon}^{t} F\left(\frac{W(\ell)}{W_1}\right) \mathrm{d}\ell \mathrm{d}\varepsilon. \end{aligned} \tag{38}$$

Differentiating ϑ_1, we obtain the following equation:

$$\begin{aligned} \frac{\mathrm{d}\vartheta_1}{\mathrm{d}t} = {} & \left(1 - \frac{X_1}{X}\right)[\rho - \alpha X - \eta XV] + \frac{1}{L_1}\left[\eta \int_0^{\infty} \overline{\mathscr{F}}_1(\varepsilon) X_{\varepsilon} V_{\varepsilon} \mathrm{d}\varepsilon - kY - vYS\right] + \frac{\eta X_1}{\wp}\left[a \int_0^{\infty} \overline{\mathscr{F}}_2(\varepsilon) Y_{\varepsilon} \mathrm{d}\varepsilon - \wp V\right] \\ & + \frac{v}{uL_1}\left(1 - \frac{S_1}{S}\right)[\xi + uYS - \gamma S - \mathfrak{F}SH] + \frac{v}{uL_1L_3}\left(1 - \frac{W_1}{W}\right)\left[\mathfrak{F} \int_0^{\infty} \overline{\mathscr{F}}_3(\varepsilon) S_{\varepsilon} H_{\varepsilon} d\varepsilon - \beta W\right] \\ & + \frac{v\beta}{u\lambda L_1L_3L_4}\left(1 - \frac{H_1}{H}\right)\left[\lambda \int_0^{\infty} \overline{\mathscr{F}}_4(\varepsilon) W_{\varepsilon} \mathrm{d}\varepsilon - \omega H\right] + \frac{\eta}{L_1} \int_0^{\infty} \overline{\mathscr{F}}_1(\varepsilon)[XV - X_{\varepsilon}V_{\varepsilon}] \mathrm{d}\varepsilon + \frac{a\eta X_1}{\wp} \int_0^{\infty} \overline{\mathscr{F}}_2(\varepsilon)[Y - Y_{\varepsilon}] \mathrm{d}\varepsilon \\ & + \frac{v\mathfrak{F}S_1H_1}{uL_1L_3} \int_0^{\infty} \overline{\mathscr{F}}_3(\varepsilon)\left[\frac{SH}{S_1H_1} - \frac{S_{\varepsilon}H_{\varepsilon}}{S_1H_1} + \ln\left(\frac{S_{\varepsilon}H_{\varepsilon}}{SH}\right)\right] \mathrm{d}\varepsilon + \frac{v\beta W_1}{uL_1L_3L_4} \int_0^{\infty} \overline{\mathscr{F}}_4(\varepsilon)\left[\frac{W}{W_1} - \frac{W_{\varepsilon}}{W_1} + \ln\left(\frac{W_{\varepsilon}}{W}\right)\right] \mathrm{d}\varepsilon. \end{aligned} \tag{39}$$

Summing the terms of equation (39), we obtain the following equation:

$$\begin{aligned} \frac{\mathrm{d}\vartheta_1}{\mathrm{d}t} = {} & \left(1 - \frac{X_1}{X}\right)(\rho - \alpha X) - \frac{1}{L_1} kY + \frac{v}{uL_1}\left(1 - \frac{S_1}{S}\right)(\xi - \gamma S) - \frac{1}{L_1} vYS_1 + \frac{v}{uL_1} \mathfrak{F}S_1H \\ & - \frac{v}{uL_1L_3} \mathfrak{F} \int_0^{\infty} \overline{\mathscr{F}}_3(\varepsilon) S_{\varepsilon} H_{\varepsilon} \frac{W_1}{W} \mathrm{d}\varepsilon + \frac{v}{uL_1L_3} \beta W_1 - \frac{v\beta}{uL_1L_3L_4} \int_0^{\infty} \overline{\mathscr{F}}_4(\varepsilon) W_{\varepsilon} \frac{H_1}{H} \mathrm{d}\varepsilon - \frac{v\beta\omega}{u\lambda L_1L_3L_4} H \\ & + \frac{v\beta\omega}{u\lambda L_1L_3L_4} H_1 + \frac{a\eta X_1}{\wp} L_2 Y + \frac{v\mathfrak{F}S_1H_1}{uL_1L_3} \int_0^{\infty} \overline{\mathscr{F}}_3(\varepsilon) \ln\left(\frac{S_{\varepsilon}H_{\varepsilon}}{SH}\right) \mathrm{d}\varepsilon + \frac{v\beta W_1}{uL_1L_3L_4} \int_0^{\infty} \overline{\mathscr{F}}_4(\varepsilon) \ln\left(\frac{W_{\varepsilon}}{W}\right) \mathrm{d}\varepsilon. \end{aligned} \tag{40}$$

By utilizing the equilibrium conditions for EP_H, we get the following equation:

$$\begin{cases} \rho = \alpha X_1, \\ \xi = \gamma S_1 + \Im H_1 S_1, \\ \Im L_3 H_1 S_1 = \beta W_1, \\ \lambda L_4 W_1 = \omega H_1. \end{cases} \tag{41}$$

Then, we obtain the following equation:

$$\begin{aligned} \frac{\mathrm{d}\vartheta_1}{\mathrm{d}t} = & -\frac{\alpha}{X}(X - X_1)^2 + \left(\frac{\eta X_1}{\wp} a L_2 - \frac{1}{L_1}k - \frac{1}{L_1}\upsilon S_1\right)Y - \frac{\upsilon\gamma}{uL_1 S}(S - S_1)^2 + \frac{\upsilon}{uL_1}\Im S_1 H_1\left(1 - \frac{S_1}{S}\right) \\ & + \frac{\upsilon}{uL_1}\Im S_1 H - \frac{\upsilon\Im S_1 H_1}{uL_1 L_3}\int_0^\infty \overline{\mathscr{L}}_3(\varepsilon)\frac{S_\varepsilon H_\varepsilon W_1}{S_1 H_1 W}\mathrm{d}\varepsilon + \frac{\upsilon}{uL_1}\Im S_1 H_1 - \frac{\upsilon\beta W_1}{uL_1 L_3 L_4}\int_0^\infty \overline{\mathscr{L}}_4(\varepsilon)\frac{W_\varepsilon H_1}{W_1 H}\mathrm{d}\varepsilon - \frac{\upsilon}{uL_1}\Im S_1 H \\ & + \frac{\upsilon}{uL_1}\Im S_1 H_1 + \frac{\upsilon\Im S_1 H_1}{uL_1 L_3}\int_0^\infty \overline{\mathscr{L}}_3(\varepsilon)\ln\left(\frac{S_\varepsilon H_\varepsilon}{SH}\right)\mathrm{d}\varepsilon + \frac{\upsilon\Im S_1 H_1}{uL_1 L_4}\int_0^\infty \overline{\mathscr{L}}_4(\varepsilon)\ln\left(\frac{W_\varepsilon}{W}\right)\mathrm{d}\varepsilon. \end{aligned} \tag{42}$$

Using the equalities given by equation (36) in case of $j = 1$, we get the following equation:

$$\begin{aligned} \frac{\mathrm{d}\vartheta_1}{\mathrm{d}t} = & -\frac{\alpha}{X}(X - X_1)^2 - \frac{\upsilon\gamma}{uL_1 S}(S - S_1)^2 + \frac{\Im k\lambda L_3 L_4 + \beta\upsilon\omega}{\Im\lambda L_1 L_3 L_4}\left(\frac{a\eta\Im\lambda\rho L_1 L_2 L_3 L_4}{\alpha\wp(\Im k\lambda L_3 L_4 + \beta\upsilon\omega)} - 1\right)Y \\ & - \frac{\upsilon}{uL_1}\Im S_1 H_1\left[\frac{S_1}{S} - 1 - \ln\left(\frac{S_1}{S}\right)\right] - \frac{\upsilon\Im S_1 H_1}{uL_1 L_3}\int_0^\infty \overline{\mathscr{L}}_3(\varepsilon)\left[\frac{S_\varepsilon H_\varepsilon W_1}{S_1 H_1 W} - 1 - \ln\left(\frac{S_\varepsilon H_\varepsilon W_1}{S_1 H_1 W}\right)\right]\mathrm{d}\varepsilon \\ & - \frac{\upsilon\Im S_1 H_1}{uL_1 L_4}\int_0^\infty \overline{\mathscr{L}}_4(\varepsilon)\left[\frac{W_\varepsilon H_1}{W_1 H} - 1 - \ln\left(\frac{W_\varepsilon H_1}{W_1 H}\right)\right]\mathrm{d}\varepsilon. \end{aligned} \tag{43}$$

Therefore, equation (43) becomes

$$\begin{aligned} \frac{\mathrm{d}\vartheta_1}{\mathrm{d}t} = & -\frac{\alpha}{X}(X - X_1)^2 - \frac{\upsilon\gamma}{uL_1 S}(S - S_1)^2 + \frac{\Im k\lambda L_3 L_4 + \beta\upsilon\omega}{\Im\lambda L_1 L_3 L_4}(R_4 - 1)Y \\ & - \frac{\upsilon}{uL_1}\Im S_1 H_1 F\left(\frac{S_1}{S}\right) - \frac{\upsilon\Im S_1 H_1}{uL_1 L_3}\int_0^\infty \overline{\mathscr{L}}_3(\varepsilon)F\left(\frac{S_\varepsilon H_\varepsilon W_1}{S_1 H_1 W}\right)\mathrm{d}\varepsilon - \frac{\upsilon\Im S_1 H_1}{uL_1 L_4}\int_0^\infty \overline{\mathscr{L}}_4(\varepsilon)F\left(\frac{W_\varepsilon H_1}{W_1 H}\right)\mathrm{d}\varepsilon. \end{aligned} \tag{44}$$

Since $R_4 \le 1$, we find that $\mathrm{d}\vartheta_1/\mathrm{d}t \le 0$ for all $X, Y, V, S, W, H > 0$. Also, $\mathrm{d}\vartheta_1/\mathrm{d}t = 0$ when $X = X_1$, $S = S_1$, $Y = 0$, $W = W_1$, and $H = H_1$. Model (2) solutions converge to T_1' the L.I.S of $T_1 = \{(X, Y, V, S, W, H)\colon \mathrm{d}\vartheta_1/\mathrm{d}t = 0\}$. The set T_1' contains elements with $Y(t) = 0$; then, $Y(t) = 0$. Second equation of system (2) implies

$$0 = \dot{Y}(t) = \eta \int_0^{\infty} \overline{\mathscr{L}}_1(\epsilon) X_1 V_{\epsilon} \mathrm{d}\epsilon, \tag{45}$$

which gives $V(t) = 0$ for all t. Therefore, $T_1' = \{EP_H\}$ and EP_H is G.A.S according to Lyapunov–LaSalle asymptotic stability theorem [40–42]. □

Theorem 3. *If $R_2 > 1$ and $R_3 \leq 1$, then the equilibrium EP_V is G.A.S.*

Proof. We introduce a Lyapunov function $\vartheta_2(X, Y, V, S, W, H)$ as follows:

$$\begin{aligned}\vartheta_2 = {} & X_2 F\left(\frac{X}{X_2}\right) + \frac{1}{L_1} Y_2 F\left(\frac{Y}{Y_2}\right) + \frac{\eta X_2}{\wp} V_2 F\left(\frac{V}{V_2}\right) + \frac{\upsilon}{uL_1} S_2 F\left(\frac{S}{S_2}\right) + \frac{\upsilon}{uL_1 L_3} W + \frac{\upsilon\beta}{u\lambda L_1 L_3 L_4} H \\ & + \frac{\eta X_2 V_2}{L_1} \int_0^{\infty} \overline{\mathscr{L}}_1(\varepsilon) \int_{t-\varepsilon}^{t} F\left(\frac{X(\ell)V(\ell)}{X_2 V_2}\right) \mathrm{d}\ell \mathrm{d}\varepsilon + \frac{a\eta X_2 Y_2}{\wp} \int_0^{\infty} \overline{\mathscr{L}}_2(\varepsilon) \int_{t-\varepsilon}^{t} F\left(\frac{Y(\ell)}{Y_2}\right) \mathrm{d}\ell \mathrm{d}\varepsilon \\ & + \frac{\upsilon}{uL_1 L_3} \mathfrak{I} \int_0^{\infty} \overline{\mathscr{L}}_3(\varepsilon) \int_{t-\varepsilon}^{t} S(\ell) H(\ell) \mathrm{d}\ell \mathrm{d}\varepsilon + \frac{\upsilon}{uL_1 L_3 L_4} \beta \int_0^{\infty} \overline{\mathscr{L}}_4(\varepsilon) \int_{t-\varepsilon}^{t} W(\ell) \mathrm{d}\ell \mathrm{d}\varepsilon.\end{aligned} \tag{46}$$

Differentiating ϑ_2, we obtain the following equation:

$$\begin{aligned}\frac{\mathrm{d}\vartheta_2}{\mathrm{d}t} = {} & \left(1 - \frac{X_2}{X}\right)[\rho - \alpha X - \eta X V] + \frac{1}{L_1}\left(1 - \frac{Y_2}{Y}\right)\left[\eta \int_0^{\infty} \overline{\mathscr{L}}_1(\varepsilon) X_{\varepsilon} V_{\varepsilon} \mathrm{d}\varepsilon - kY - \upsilon Y S\right] + \frac{\eta X_2}{\wp}\left(1 - \frac{V_2}{V}\right) \\ & \times \left[a \int_0^{\infty} \overline{\mathscr{L}}_2(\varepsilon) Y_{\varepsilon} \mathrm{d}\varepsilon - \wp V\right] + \frac{\upsilon}{uL_1}\left(1 - \frac{S_2}{S}\right)[\xi + uYS - \gamma S - \mathfrak{I} S H] + \frac{\upsilon}{uL_1 L_3}\left[\mathfrak{I} \int_0^{\infty} \overline{\mathscr{L}}_3(\varepsilon) S_{\varepsilon} H_{\varepsilon} \mathrm{d}\varepsilon - \beta W\right] \\ & + \frac{\upsilon\beta}{u\lambda L_1 L_3 L_4}\left[\lambda \int_0^{\infty} \overline{\mathscr{L}}_4(\varepsilon) W_{\varepsilon} \mathrm{d}\varepsilon - \omega H\right] + \frac{\eta X_2 V_2}{L_1} \int_0^{\infty} \overline{\mathscr{L}}_1(\varepsilon)\left[\frac{XV}{X_2 V_2} - \frac{X_{\varepsilon} V_{\varepsilon}}{X_2 V_2} + \ln\left(\frac{X_{\varepsilon} V_{\varepsilon}}{XV}\right)\right] \mathrm{d}\varepsilon \\ & + \frac{a\eta X_2 Y_2}{\wp} \int_0^{\infty} \overline{\mathscr{L}}_2(\varepsilon)\left[\frac{Y}{Y_2} - \frac{Y_{\varepsilon}}{Y_2} + \ln\left(\frac{Y_{\varepsilon}}{Y}\right)\right] \mathrm{d}\varepsilon + \frac{\upsilon}{uL_1 L_3} \mathfrak{I} \int_0^{\infty} \overline{\mathscr{L}}_3(\varepsilon)[SH - S_{\varepsilon} H_{\varepsilon}] \mathrm{d}\varepsilon \\ & + \frac{\upsilon\beta}{uL_1 L_3 L_4} \int_0^{\infty} \overline{\mathscr{L}}_4(\varepsilon)[W - W_{\varepsilon}] \mathrm{d}\varepsilon.\end{aligned} \tag{47}$$

By collecting the terms of equation (47), we have the following equation:

$$\begin{aligned}\frac{\mathrm{d}\vartheta_2}{\mathrm{d}t} = {} & \left(1 - \frac{X_2}{X}\right)(\rho - \alpha X) - \frac{\eta}{L_1} \int_0^{\infty} \overline{\mathscr{L}}_1(\varepsilon) X_{\varepsilon} V_{\varepsilon} \frac{Y_2}{Y} d\varepsilon - \frac{1}{L_1} kY + \frac{1}{L_1} kY_2 + \frac{1}{L_1} \upsilon Y_2 S - \frac{\eta X_2}{\wp} a \int_0^{\infty} \overline{\mathscr{L}}_2(\varepsilon) Y_{\varepsilon} \frac{V_2}{V} \mathrm{d}\varepsilon \\ & + \eta X_2 V_2 + \frac{\upsilon}{uL_1}\left(1 - \frac{S_2}{S}\right)(\xi - \gamma S) - \frac{1}{L_1} \upsilon Y S_2 + \frac{\upsilon}{uL_1} \mathfrak{I} S_2 H - \frac{\upsilon\beta\omega}{u\lambda L_1 L_3 L_4} H + \frac{\eta X_2 V_2}{L_1} \int_0^{\infty} \overline{\mathscr{L}}_1(\varepsilon) \ln\left(\frac{X_{\varepsilon} V_{\varepsilon}}{XV}\right) \mathrm{d}\varepsilon \\ & + \frac{a\eta X_2}{\wp} L_2 Y + \frac{a\eta X_2 Y_2}{\wp} \int_0^{\infty} \overline{\mathscr{L}}_2(\varepsilon) \ln\left(\frac{Y_{\varepsilon}}{Y}\right) \mathrm{d}\varepsilon.\end{aligned} \tag{48}$$

By using the equilibrium conditions for EP_V,

$$\begin{cases} \rho = \alpha X_2 + \eta X_2 V_2, \\ \eta L_1 X_2 V_2 = k Y_2 + \upsilon Y_2 S_2, \\ a L_2 Y_2 = \wp V_2, \\ \xi = \gamma S_2 - u Y_2 S_2, \end{cases} \tag{49}$$

we obtain the following equation:

$$\begin{aligned} \frac{\mathrm{d}\vartheta_2}{\mathrm{d}t} &= -\frac{\alpha}{X}(X - X_2)^2 + \eta V_2 X_2\left(1 - \frac{X_2}{X}\right) + \left(\frac{\eta X_2}{\wp} a L_2 - \frac{1}{L_1}k - \frac{1}{L_1}\upsilon S_2\right)Y - \frac{\eta X_2 V_2}{L_1}\int_0^\infty \overline{\mathscr{L}}_1(\varepsilon)\frac{X_\varepsilon V_\varepsilon Y_2}{X_2 V_2 Y}\mathrm{d}\varepsilon \\ &+ \eta X_2 V_2 - \frac{1}{L_1}\upsilon Y_2 S_2 + \frac{1}{L_1}\upsilon Y_2 S - \frac{a\eta X_2 Y_2}{\wp}\int_0^\infty \overline{\mathscr{L}}_2(\varepsilon)\frac{Y_\varepsilon V_2}{Y_2 V}\mathrm{d}\varepsilon + \eta X_2 V_2 - \frac{\upsilon\gamma}{u L_1 S}(S - S_2)^2 - \frac{1}{L_1}\upsilon Y_2 S_2\left(1 - \frac{S_2}{S}\right) \\ &+ \frac{\upsilon}{u L_1}\left(\mathfrak{F} S_2 - \frac{\beta\omega}{\lambda L_3 L_4}\right)H + \frac{\eta X_2 V_2}{L_1}\int_0^\infty \overline{\mathscr{L}}_1(\varepsilon)\ln\left(\frac{X_\varepsilon V_\varepsilon}{XV}\right)\mathrm{d}\varepsilon + \frac{\eta X_2 V_2}{L_2}\int_0^\infty \overline{\mathscr{L}}_2(\varepsilon)\ln\left(\frac{Y_\varepsilon}{Y}\right)\mathrm{d}\varepsilon. \end{aligned} \tag{50}$$

Using the equalities given by equation (37) in case of $i = 2$, we get the following equation:

$$\begin{aligned} \frac{\mathrm{d}\vartheta_2}{\mathrm{d}t} &= -\frac{\alpha}{X}(X - X_2)^2 - \frac{\upsilon\gamma}{u L_1 S}(S - S_2)^2 - \frac{1}{L_1}\upsilon Y_2 S_2\left(2 - \frac{S_2}{S} - \frac{S}{S_2}\right) - \eta X_2 V_2\left[\frac{X_2}{X} - 1 - \ln\left(\frac{X_2}{X}\right)\right] \\ &+ \frac{\upsilon}{u L_1}\left(\mathfrak{F} S_2 - \frac{\beta\omega}{\lambda L_3 L_4}\right)H - \frac{\eta X_2 V_2}{L_1}\int_0^\infty \overline{\mathscr{L}}_1(\varepsilon)\left[\frac{X_\varepsilon V_\varepsilon Y_2}{X_2 V_2 Y} - 1 - \ln\left(\frac{X_\varepsilon V_\varepsilon Y_2}{X_2 V_2 Y}\right)\right]\mathrm{d}\varepsilon \\ &- \frac{\eta X_2 V_2}{L_2}\int_0^\infty \overline{\mathscr{L}}_2(\varepsilon)\left[\frac{Y_\varepsilon V_2}{Y_2 V} - 1 - \ln\left(\frac{Y_\varepsilon V_2}{Y_2 V}\right)\right]\mathrm{d}\varepsilon. \end{aligned} \tag{51}$$

Therefore, equation (51) becomes

$$\begin{aligned} \frac{\mathrm{d}\vartheta_2}{\mathrm{d}t} &= -\frac{\alpha}{X}(X - X_2)^2 - \frac{\upsilon\xi}{u L_1 S S_2}(S - S_2)^2 - \eta X_2 V_2 F\left(\frac{X_2}{X}\right) + \frac{\upsilon}{u L_1}\left(\mathfrak{F} S_2 - \frac{\beta\omega}{\lambda L_3 L_4}\right)H \\ &- \frac{\eta X_2 V_2}{L_1}\int_0^\infty \overline{\mathscr{L}}_1(\varepsilon)F\left(\frac{X_\varepsilon V_\varepsilon Y_2}{X_2 V_2 Y}\right)\mathrm{d}\varepsilon - \frac{\eta X_2 V_2}{L_2}\int_0^\infty \overline{\mathscr{L}}_2(\varepsilon)F\left(\frac{Y_\varepsilon V_2}{Y_2 V}\right)\mathrm{d}\varepsilon. \end{aligned} \tag{52}$$

If $R_3 \le 1$, then Ep_{VH} does not exist since $H_3 \le 0$ and $W_3 \le 0$. This implies that

$$\begin{aligned} \dot{H}(t) &= \lambda L_4 W - \omega H \le 0, \\ \dot{W}(t) &= \mathfrak{F} L_3 S H - \beta W \le 0. \end{aligned} \tag{53}$$

Therefore, we get $(\mathfrak{F}S - \beta\omega/\lambda L_3 L_4)H \le 0$ for all $H, S > 0$. Hence, we have $(\mathfrak{F}S_2 - \beta\omega/\lambda L_3 L_4) \le 0$, and therefore, $\mathrm{d}\vartheta_2/\mathrm{d}t \le 0$ for all $X, Y, V, S, W, H > 0$. In addition, $\mathrm{d}\vartheta_2/\mathrm{d}t = 0$ when $X = X_2$, $S = S_2$, $H = 0$, $Y = Y_2$, and $V = V_2$. Solutions of the model (2) that converge to T_2' is the L.I.S of $\mathrm{T}_2 = \{(X, Y, V, S, W, H)\colon \mathrm{d}\vartheta_2/\mathrm{d}t = 0\}$. The set T_2' has elements with $H(t) = 0$, and thus, $\dot{H}(t) = 0$. Using system (2) last equation, we get the following equation:

$$0 = \dot{H}(t) = \lambda\int_0^\infty \overline{\mathscr{L}}_4(\epsilon)W_\epsilon d\epsilon. \tag{54}$$

Yield $W(t) = 0$ for all values of t. Therefore, $T_2' = \{EP_V\}$ and EP_V is G.A.S according to Lyapunov–LaSalle asymptotic stability theorem [40–42]. □

Theorem 4. *If* $R_4 > 1$ *and* $1 < R_3 \leq 1 + a\eta\Im\lambda\xi L_2L_3L_4/\beta\omega(u\alpha\wp + a\gamma\eta L_2)$, *then the equilibrium* EP_{VH} *is G.A.S.*

Proof. We consider a Lyapunov function $\vartheta_3(X, Y, V, S, W, H)$ as follows:

$$\begin{aligned}\vartheta_3 = {} & X_3F\left(\frac{X}{X_3}\right) + \frac{1}{L_1}Y_3F\left(\frac{Y}{Y_3}\right) + \frac{\eta X_3}{\wp}V_3F\left(\frac{V}{V_3}\right) + \frac{\upsilon}{uL_1}S_3F\left(\frac{S}{S_3}\right) + \frac{\upsilon}{uL_1L_3}W_3F\left(\frac{W}{W_3}\right)\\ & + \frac{\upsilon\beta}{u\lambda L_1L_3L_4}H_3F\left(\frac{H}{H_3}\right) + \frac{\eta X_3V_3}{L_1}\int_0^\infty \overline{\mathscr{L}}_1(\varepsilon)\int_{t-\varepsilon}^t F\left(\frac{X(\ell)V(\ell)}{X_3V_3}\right)\mathrm{d}\ell\mathrm{d}\varepsilon + \frac{a\eta X_3Y_3}{\wp}\int_0^\infty \overline{\mathscr{L}}_2(\varepsilon)\int_{t-\varepsilon}^t F\left(\frac{Y(\ell)}{Y_3}\right)\mathrm{d}\ell\mathrm{d}\varepsilon\\ & + \frac{\upsilon\Im S_3H_3}{uL_1L_3}\int_0^\infty \overline{\mathscr{L}}_3(\varepsilon)\int_{t-\varepsilon}^t F\left(\frac{S(\ell)H(\ell)}{S_3H_3}\right)\mathrm{d}\ell\mathrm{d}\varepsilon + \frac{\upsilon\beta W_3}{uL_1L_3L_4}\int_0^\infty \overline{\mathscr{L}}_4(\varepsilon)\int_{t-\varepsilon}^t F\left(\frac{W(\ell)}{W_3}\right)\mathrm{d}\ell\mathrm{d}\varepsilon.\end{aligned} \tag{55}$$

By differentiating ϑ_3, we obtain the following equation:

$$\begin{aligned}\frac{\mathrm{d}\vartheta_3}{\mathrm{d}t} = {} & \left(1 - \frac{X_3}{X}\right)[\rho - \alpha X - \eta XV] + \frac{1}{L_1}\left(1 - \frac{Y_3}{Y}\right)\left[\eta\int_0^\infty \overline{\mathscr{L}}_1(\varepsilon)X_\varepsilon V_\varepsilon d\varepsilon - kY - \upsilon YS\right] + \frac{\eta X_3}{\wp}\left(1 - \frac{V_3}{V}\right)\\ & \times\left[a\int_0^\infty \overline{\mathscr{L}}_2(\varepsilon)Y_\varepsilon\mathrm{d}\varepsilon - \wp V\right] + \frac{\upsilon}{uL_1}\left(1 - \frac{S_3}{S}\right)[\xi + uYS - \gamma S - \Im SH] + \frac{\upsilon}{uL_1L_3}\left(1 - \frac{W_3}{W}\right)\\ & \times\left[\Im\int_0^\infty \overline{\mathscr{L}}_3(\varepsilon)S_\varepsilon H_\varepsilon\mathrm{d}\varepsilon - \beta W\right] + \frac{\upsilon\beta}{u\lambda L_1L_3L_4}\left(1 - \frac{H_3}{H}\right)\left[\lambda\int_0^\infty \overline{\mathscr{L}}_4(\varepsilon)W_\varepsilon\mathrm{d}\varepsilon - \omega H\right]\\ & + \frac{\eta X_3V_3}{L_1}\int_0^\infty \overline{\mathscr{L}}_1(\varepsilon)\left[\frac{XV}{X_3V_3} - \frac{X_\varepsilon V_\varepsilon}{X_3V_3} + \ln\left(\frac{X_\varepsilon V_\varepsilon}{XV}\right)\right]\mathrm{d}\varepsilon + \frac{a\eta X_3Y_3}{\wp}\int_0^\infty \overline{\mathscr{L}}_2(\varepsilon)\left[\frac{Y}{Y_3} - \frac{Y_\varepsilon}{Y_3} + \ln\left(\frac{Y_\varepsilon}{Y}\right)\right]\mathrm{d}\varepsilon\\ & + \frac{\upsilon\Im S_3H_3}{uL_1L_3}\int_0^\infty \overline{\mathscr{L}}_3(\varepsilon)\left[\frac{SH}{S_3H_3} - \frac{S_\varepsilon H_\varepsilon}{S_3H_3} + \ln\left(\frac{S_\varepsilon H_\varepsilon}{SH}\right)\right]\mathrm{d}\varepsilon + \frac{\upsilon\beta W_3}{uL_1L_3L_4}\int_0^\infty \overline{\mathscr{L}}_4(\varepsilon)\left[\frac{W}{W_3} - \frac{W_\varepsilon}{W_3} + \ln\left(\frac{W_\varepsilon}{W}\right)\right]\mathrm{d}\varepsilon.\end{aligned} \tag{56}$$

Collecting terms of equation (56) gives the following equation:

$$\begin{aligned}\frac{\mathrm{d}\vartheta_3}{\mathrm{d}t} = {} & \left(1 - \frac{X_3}{X}\right)(\rho - \alpha X) - \frac{\eta}{L_1}\int_0^\infty \overline{\mathscr{L}}_1(\varepsilon)X_\varepsilon V_\varepsilon\frac{Y_3}{Y}d\varepsilon - \frac{1}{L_1}kY + \frac{1}{L_1}kY_3 + \frac{1}{L_1}\upsilon Y_3S - \frac{\eta X_3}{\wp}a\int_0^\infty \overline{\mathscr{L}}_2(\varepsilon)Y_\varepsilon\frac{V_3}{V}\mathrm{d}\varepsilon\\ & + \eta X_3V_3 + \frac{\upsilon}{uL_1}\left(1 - \frac{S_3}{S}\right)(\xi - \gamma S) - \frac{1}{L_1}\upsilon YS_3 + \frac{\upsilon}{uL_1}\Im S_3H - \frac{\upsilon}{uL_1L_3}\Im\int_0^\infty \overline{\mathscr{L}}_3(\varepsilon)S_\varepsilon H_\varepsilon\frac{W_3}{W}\mathrm{d}\varepsilon + \frac{\upsilon}{uL_1L_3}\beta W_3\\ & - \frac{\upsilon\beta}{uL_1L_3L_4}\int_0^\infty \overline{\mathscr{L}}_4(\varepsilon)W_\varepsilon\frac{H_3}{H}\mathrm{d}\varepsilon - \frac{\upsilon\beta}{u\lambda L_1L_3L_4}\omega H + \frac{\upsilon\beta}{u\lambda L_1L_3L_4}\omega H_3 + \frac{\eta X_3V_3}{L_1}\int_0^\infty \overline{\mathscr{L}}_1(\varepsilon)\ln\left(\frac{X_\varepsilon V_\varepsilon}{XV}\right)\mathrm{d}\varepsilon\\ & + \frac{a\eta X_3}{\wp}L_2Y + \frac{a\eta X_3Y_3}{\wp}\int_0^\infty \overline{\mathscr{L}}_2(\varepsilon)\ln\left(\frac{Y_\varepsilon}{Y}\right)\mathrm{d}\varepsilon + \frac{\upsilon\Im S_3H_3}{uL_1L_3}\int_0^\infty \overline{\mathscr{L}}_3(\varepsilon)\ln\left(\frac{S_\varepsilon H_\varepsilon}{SH}\right)\mathrm{d}\varepsilon\\ & + \frac{\upsilon\beta W_3}{uL_1L_3L_4}\int_0^\infty \overline{\mathscr{L}}_4(\varepsilon)\ln\left(\frac{W_\varepsilon}{W}\right)\mathrm{d}\varepsilon.\end{aligned} \tag{57}$$

By using the equilibrium conditions for EP_{VH},

$$\begin{cases} \rho = \alpha X_3 + \eta V_3 X_3, \\ \eta L_1 V_3 X_3 = kY_3 + \upsilon Y_3 S_3, \\ aL_2 Y_3 = \wp V_3, \\ \xi = \gamma S_3 + \mathfrak{I} H_3 S_3 - \iota Y_3 S_3, \\ \mathfrak{I} L_3 H_3 S_3 = \beta W_3, \\ \lambda L_4 W_3 = \omega H_3, \end{cases} \tag{58}$$

we get the following equation:

$$\begin{aligned} \frac{\mathrm{d}\vartheta_3}{\mathrm{d}t} &= -\frac{\alpha}{X}(X - X_3)^2 + \eta V_3 X_3\left(1 - \frac{X_3}{X}\right) + \left(\frac{\eta X_3}{\wp} aL_2 - \frac{1}{L_1}k - \frac{1}{L_1}\upsilon S_3\right)Y - \frac{\eta X_3 V_3}{L_1}\int_0^\infty \overline{\mathscr{L}}_1(\varepsilon)\frac{X_\varepsilon V_\varepsilon Y_3}{X_3 V_3 Y}\mathrm{d}\varepsilon \\ &+ \eta X_3 V_3 - \frac{1}{L_1}\upsilon Y_3 S_3 + \frac{1}{L_1}\upsilon Y_3 S - \frac{\eta X_3 Y_3}{\wp} a\int_0^\infty \overline{\mathscr{L}}_2(\varepsilon)\frac{Y_\varepsilon V_3}{Y_3 V}\mathrm{d}\varepsilon + \eta X_3 V_3 - \frac{\upsilon\gamma}{\iota L_1 S}(S - S_3)^2 \\ &- \frac{1}{L_1}\upsilon Y_3 S_3\left(1 - \frac{S_3}{S}\right) + \frac{\upsilon}{\iota L_1}\mathfrak{I} S_3 H_3\left(1 - \frac{S_3}{S}\right) + \frac{\upsilon}{\iota L_1}\mathfrak{I} S_3 H - \frac{\upsilon\mathfrak{I} S_3 H_3}{\iota L_1 L_3}\int_0^\infty \overline{\mathscr{L}}_3(\varepsilon)\frac{S_\varepsilon H_\varepsilon W_3}{S_3 H_3 W}\mathrm{d}\varepsilon \\ &+ \frac{\upsilon}{\iota L_1}\mathfrak{I} S_3 H_3 - \frac{\upsilon\beta W_3}{\iota L_1 L_3 L_4}\int_0^\infty \overline{\mathscr{L}}_4(\varepsilon)\frac{W_\varepsilon H_3}{W_3 H}\mathrm{d}\varepsilon - \frac{\upsilon}{\iota L_1}\mathfrak{I} S_3 H + \frac{\upsilon}{\iota L_1}\mathfrak{I} S_3 H_3 + \frac{\eta X_3 V_3}{L_1}\int_0^\infty \overline{\mathscr{L}}_1(\varepsilon)\ln\left(\frac{X_\varepsilon V_\varepsilon}{XV}\right)\mathrm{d}\varepsilon \\ &+ \frac{\eta X_3 V_3}{L_2}\int_0^\infty \overline{\mathscr{L}}_2(\varepsilon)\ln\left(\frac{Y_\varepsilon}{Y}\right)\mathrm{d}\varepsilon + \frac{\upsilon\mathfrak{I} S_3 H_3}{\iota L_1 L_3}\int_0^\infty \overline{\mathscr{L}}_3(\varepsilon)\ln\left(\frac{S_\varepsilon H_\varepsilon}{SH}\right)\mathrm{d}\varepsilon + \frac{\upsilon\mathfrak{I} S_3 H_3}{\iota L_1 L_4}\int_0^\infty \overline{\mathscr{L}}_4(\varepsilon)\ln\left(\frac{W_\varepsilon}{W}\right)\mathrm{d}\varepsilon. \end{aligned} \tag{59}$$

Using the equalities given by equations (36) and (37) in case of $i, j = 3$, we get the following equation:

$$\begin{aligned} \frac{\mathrm{d}\vartheta_3}{\mathrm{d}t} &= -\frac{\alpha}{X}(X - X_3)^2 - \frac{\upsilon\gamma}{\iota L_1 S}(S - S_3)^2 - \frac{1}{L_1}\upsilon Y_3 S_3\left(2 - \frac{S_3}{S} - \frac{S}{S_3}\right) - \eta X_3 V_3\left[\frac{X_3}{X} - 1 - \ln\left(\frac{X_3}{X}\right)\right] \\ &- \frac{\upsilon\mathfrak{I} S_3 H_3}{\iota L_1}\left[\frac{S_3}{S} - 1 - \ln\left(\frac{S_3}{S}\right)\right] - \frac{\eta X_3 V_3}{L_1}\int_0^\infty \overline{\mathscr{L}}_1(\varepsilon)\left[\frac{X_\varepsilon V_\varepsilon Y_3}{X_3 V_3 Y} - 1 - \ln\left(\frac{X_\varepsilon V_\varepsilon Y_3}{X_3 V_3 Y}\right)\right]\mathrm{d}\varepsilon \\ &- \frac{\eta X_3 V_3}{L_2} a\int_0^\infty \overline{\mathscr{L}}_2(\varepsilon)\left[\frac{Y_\varepsilon V_3}{Y_3 V} - 1 - \ln\left(\frac{Y_\varepsilon V_3}{Y_3 V}\right)\right]\mathrm{d}\varepsilon - \frac{\upsilon\mathfrak{I} S_3 H_3}{\iota L_1 L_3}\int_0^\infty \overline{\mathscr{L}}_3(\varepsilon)\left[\frac{S_\varepsilon H_\varepsilon W_3}{S_3 H_3 W} - 1 - \ln\left(\frac{S_\varepsilon H_\varepsilon W_3}{S_3 H_3 W}\right)\right]\mathrm{d}\varepsilon \\ &- \frac{\upsilon\mathfrak{I} S_3 H_3}{\iota L_1 L_4}\int_0^\infty \overline{\mathscr{L}}_4(\varepsilon)\left[\frac{W_\varepsilon H_3}{W_3 H} - 1 - \ln\left(\frac{W_\varepsilon H_3}{W_3 H}\right)\right]\mathrm{d}\varepsilon. \end{aligned} \tag{60}$$

Therefore, equation (60) becomes the following equation:

$$\begin{aligned}\frac{\mathrm{d}\vartheta_3}{\mathrm{d}t} &= -\frac{\alpha}{X}(X-X_3)^2 + \frac{\upsilon(u\alpha\wp + a\gamma\eta L_2)}{a\eta u S L_1 L_2}(S-S_3)^2\left(\frac{a\eta\Im u\lambda\rho L_1L_2L_3L_4}{(\Im k\lambda L_3L_4+\beta\upsilon\omega)(u\alpha\wp+a\gamma\eta L_2)}-1\right) - \eta X_3V_3F\left(\frac{X_3}{X}\right)\\ &- \frac{\upsilon\Im S_3H_3}{uL_1}F\left(\frac{S_3}{S}\right) - \frac{\eta X_3V_3}{L_1}\int_0^\infty \overline{\mathscr{L}}_1(\varepsilon)F\left(\frac{X_\varepsilon V_\varepsilon Y_3}{X_3V_3Y}\right)\mathrm{d}\varepsilon - \frac{\eta X_3V_3}{L_2}\int_0^\infty \overline{\mathscr{L}}_2(\varepsilon)F\left(\frac{Y_\varepsilon V_3}{Y_3V}\right)\mathrm{d}\varepsilon\\ &- \frac{\upsilon\Im S_3H_3}{uL_1L_3}\int_0^\infty \overline{\mathscr{L}}_3(\varepsilon)F\left(\frac{S_\varepsilon H_\varepsilon W_3}{S_3H_3W}\right)\mathrm{d}\varepsilon - \frac{\upsilon\Im S_3H_3}{uL_1L_4}\int_0^\infty \overline{\mathscr{L}}_4(\varepsilon)F\left(\frac{W_\varepsilon H_3}{W_3H}\right)\mathrm{d}\varepsilon.\end{aligned} \tag{61}$$

Since $1 < R_3 \le 1 + a\eta\Im\lambda\xi L_2L_3L_4/\beta\omega(u\alpha\wp + a\gamma\eta L_2)$, then $\mathrm{d}\vartheta_3/\mathrm{d}t \le 0$ for the positive values of X, Y, V, S, W, and H. Moreover, $\mathrm{d}\vartheta_3/\mathrm{d}t = 0$ when $X = X_3$, $S = S_3$, $Y(t) = Y_3$, $V(t) = V_3$, $W(t) = W_3$, and $H(t) = H_3$. The model trajectories that converge to T_3' be the L.I.S of $T_3 = \{(X, Y, V, S, W, H)\colon \mathrm{d}\vartheta_3/dt = 0\}$. Hence, $T_3' = \{EP_{VH}\}$ and EP_{VH} is G.A.S according to Lyapunov–LaSalle stability theorem. □

All equilibria of model (2) with the existence conditions and global stability constraints are summarized in Table 1.

5. Numerical Simulations

We execute numerical simulations in this part to enhance the outcomes of Theorems 1–4. Moreover, the impact of time delays on system dynamical behavior will be tested. To transform a model with distributed time delay (2) to a discrete one, we choose a Dirac delta function $D(.)$ as a specific formula of kernel $g_i(.)$ as follows:

$$g_i(\nu) = D(\nu - \varepsilon_i), \quad \varepsilon_i \in [0,\infty), \quad i = 1,2,3,4. \tag{62}$$

Then, we get the following equation:

$$L_j = \int_0^\infty D(\varsigma - \epsilon_j)e^{-m_j\varsigma}\mathrm{d}\varsigma = e^{-m_j\epsilon_j}, \quad j = 1,2,3,4. \tag{63}$$

Thus, model (2) is reduced as follows:

$$\begin{cases}\dot{X}(t) = \rho - \alpha X(t) - \eta X(t)V(t),\\ \dot{Y}(t) = \eta e^{-m_1\epsilon_1}X(t-\epsilon_1)V(t-\epsilon_1) - kY(t) - \upsilon Y(t)S(t),\\ \dot{V}(t) = ae^{-m_2\epsilon_2}Y(t-\epsilon_2) - \wp V(t),\\ \dot{S}(t) = \xi + uY(t)S(t) - \gamma S(t) - \Im S(t)H(t),\\ \dot{W}(t) = \Im e^{-m_3\epsilon_3}S(t-\epsilon_3)H(t-\epsilon_3) - \beta W(t),\\ \dot{H}(t) = \lambda e^{-m_4\epsilon_4}W(t-\epsilon_4) - \omega H(t).\end{cases} \tag{64}$$

For model (64), the threshold parameters are given by the following equation:

$$\begin{cases} R_1 = \dfrac{\xi\Im\lambda e^{-(m_3\epsilon_3+m_4\epsilon_4)}}{\beta\gamma\omega},\\ R_2 = \dfrac{a\gamma\eta\rho e^{-(m_1\epsilon_1+m_2\epsilon_2)}}{\alpha\wp(\gamma k+\upsilon\xi)},\\ R_3 = \left(\dfrac{\lambda\xi}{\beta\omega} + \dfrac{u\lambda\rho e^{-m_1\epsilon_1}}{\Im k\lambda e^{-(m_3\epsilon_3+m_4\epsilon_4)}+\beta\upsilon\omega}\right)\dfrac{a\eta\Im e^{-(m_2\epsilon_2+m_3\epsilon_3+m_4\epsilon_4)}}{u\alpha\wp + a\gamma\eta e^{-m_2\epsilon_2}},\\ R_4 = \dfrac{a\eta\Im\lambda\rho e^{-(m_1\epsilon_1+m_2\epsilon_2+m_3\epsilon_3+m_4\epsilon_4)}}{\alpha\wp\left[\Im k\lambda e^{-(m_3\epsilon_3+m_4\epsilon_4)}+\beta\upsilon\omega\right]}.\end{cases} \tag{65}$$

To solve system (18) numerically, we change some parameters values whilst assigning fixed estimate to the rest parameters (Table 2). We modify the parameters $\eta, \upsilon, \wp$, and $\Im$ to test the conclusions of Theorems 1–4. Furthermore, to test the impact of the time delays upon COVID-19/AIDS dynamics, delays parameters $\epsilon_1, \epsilon_2, \epsilon_3$, and ϵ_4 have been changed.

5.1. Stability of Equilibrium Points. During this part, we choose delay parameters as follows: $\epsilon_1 = 1$, $\epsilon_2 = 0.8$, $\epsilon_3 = 1$, and $\epsilon_4 = 0.8$. Additionally, we select three distinct starting conditions of the model (18):

Initial-1: $X(\epsilon) = 5$, $Y(\epsilon) = 0.0001$, $V(\epsilon) = 0.0002$, $S(\epsilon) = 100$, $W(\epsilon) = 5$, and $H(\epsilon) = 10$,

Initial-2: $X(\epsilon) = 10$, $Y(\epsilon) = 0.001$, $V(\epsilon) = 0.002$, $S(\epsilon) = 200$, $W(\epsilon) = 10$, and $H(\epsilon) = 15$,

Initial-3: $X(\epsilon) = 15$, $Y(\epsilon) = 0.002$, $V(\epsilon) = 0.003$, $S(\epsilon) = 300$, $W(\epsilon) = 15$, and $H(\epsilon) = 20$.

Here, $\epsilon \in [-\max\{\epsilon_1, \epsilon_2, \epsilon_3, \epsilon_4\}, 0]$ and it is optional to pick these values. Moreover, the initial conditions are split into three groups to provide global stability for any starting conditions. To dissolve system (18), we utilize MATLAB solver dde23. Based on equilibrium points EP_0, EP_H, EP_V, and EP_{VH} global stability explained in Theorems 1–4, the simulations are divided into four cases. In these instances, we change values of η, υ, $\wp$, and $\Im$ of system (18). Other

Table 1: Equilibrium points of model (2), existence conditions, and global stability conditions.

Equilibrium	Existence conditions	Global stability conditions
$EP_0 = (X_0, 0, 0, S_0, 0, 0)$	None	$R_1 \le 1$ and $R_2 \le 1$
$EP_H = (X_1, 0, 0, S_1, W_1, H_1)$	$R_1 > 1$	$R_1 > 1$ and $R_4 \le 1$
$EP_V = (X_2, Y_2, V_2, S_2, 0, 0)$	$R_2 > 1$	$R_2 > 1$ and $R_3 \le 1$
$EP_{VH} = (X_3, Y_3, V_3, S_3, W_3, H_3)$	$R_3 > 1$ and $R_4 > 1$	$R_4 > 1$ and $1 < R_3 \le 1 + (a\eta\mathfrak{J}\lambda\xi L_2 L_3 L_4)/(\beta\omega(u\alpha\wp + a\gamma\eta L_2))$

Table 2: Model (64) parameter values.

Parameters	Value	Reference
ρ	0.02241	[24]
α	10^{-3}	[24]
η	Varied	—
k	0.11	[24]
υ	Varied	—
a	0.24	[24]
$\wp$	Varied	—
ξ	10	[19]
u	0.1	[44]
γ	0.01	[45]
$\mathfrak{J}$	Varied	—
β	0.5	[43]
λ	5	[35]
ω	2	[35]
m_1	0.1	—
m_2	0.2	—
m_3	0.2	—
m_4	0.3	—
$\epsilon_i, i = 1, \ldots, 4$	Varied	—

parameters values are set and recorded in Table 2. The four scenarios are detailed as follows:

(i) Case 1 (stability of EP_0): we take $\eta = 0.006$, $\upsilon = 0.01$, $\wp = 0.3$, and $\mathfrak{J} = 0.0001$. The thresholds in this case are given by $R_1 = 0.322 < 1$ and $R_2 = 0.008 < 1$. In harmony with Theorem 1, the equilibrium $EP_0 = (22.41, 0, 0, 1000, 0, 0)$ is G.A.S (Figure 2). This is the best case scenario when the person is free of SARS-CoV-2 and HIV-1 infection.

(ii) Case 2 (stability of EP_H): we get $\eta = 0.0006$, $\upsilon = 0.01$, $\wp = 0.3$, and $\mathfrak{J} = 0.0016$. This provides us with $R_1 = 5.15 > 1$ and $R_4 = 0.004 < 1$. According to Theorem 2, the equilibrium $EP_H = (22.41, 0, 0, 186.478, 13.3211, 27.266)$ is G.A.S (Figure 3). This simulates the situation in which a person has HIV-1 infection with depressed $CD4^+$ T cell levels, but SARS-CoV-2 infection is not present.

(iii) Case 3 (stability of EP_V): we select $\eta = 2.9$, $\upsilon = 0.002$, $\wp = 0.1$, and $\mathfrak{J} = 0.0001$. This gives $R_2 = 56.997 > 1$ and $R_3 = 0.3535 < 1$. In this situation, the system solutions converge globally to equilibrium $EP_V = (0.4285, 0.0087, 0.018, 1094.69, 0, 0)$. This result accords with Theorem 3 (Figure 4). This scenario simulates the case of a person infected with SARS-CoV-2 but not HIV-1 infection.

(iv) Case 4 (stability of EP_{VH}): we consider $\eta = 2.9$, $\upsilon = 0.02$, $\wp = 0.1$, and $\mathfrak{J} = 0.0016$. This implies that $R_3 = 5.19433 > 1$, $R_3 < 1 + a\eta\mathfrak{J}\lambda\xi L_2 L_3 L_4/\beta\omega(u\alpha\wp + a\gamma\eta L_2) = 6.1436$, and $R_4 = 30.1279 > 1$. In agreement with Theorem 4, the equilibrium $EP_{VH} = (0.7155, 0.005, 0.0105, 186.478, 13.48, 27.59)$ is G.A.S (Figure 5). In this case, COVID-19/AIDS coinfection occurs, where an HIV-1 patient gets infected with SARS-CoV-2. $CD4^+$ T cells, which are the main target of HIV-1, are recruited to eliminate SARS-CoV-2 infection from the body. However, if the patient has low $CD4^+$ T cell counts, the clearance of SARS-CoV-2 may not be achieved. This can cause severe infection and death.

5.2. Impact of Time Delays on COVID-19/AIDS Dynamics. Here, we adjust parameters of delay $\epsilon_i, i = 1, 2, \ldots, 4$ and set the parameters values $\eta = 2.9, \upsilon = 0.02, \wp = 0.1$, and $\mathfrak{J} = 0.0016$. Since R_1, R_2, R_3, and R_4 offered by equation (65) rely on $\epsilon_i, i = 1, 2, \ldots, 4$, varying parameters ϵ_i will convert stability of the equilibria. We consider the following cases:

(D.P.S1) $\epsilon_1 = \epsilon_2 = \epsilon_3 = \epsilon_4 = 0$

(D.P.S2) $\epsilon_1 = 0.3, \epsilon_2 = 0.4, \epsilon_3 = 0.5$, and $\epsilon_4 = 0.6$

(D.P.S3) $\epsilon_1 = 10, \epsilon_2 = 11, \epsilon_3 = 12$, and $\epsilon_4 = 13$

With the above values, we solve model (64) with given initial conditions:

Initial-3: $(X(\epsilon), Y(\epsilon), V(\epsilon), S(\epsilon), W(\epsilon), H(\epsilon)) = (15, 0.002, 0.003, 300, 15, 20)$.

The inclusion of time delays can increase the number of uninfected epithelial and CD4+ T cells while diminish the number of other compartments, as shown in Figure 6. Table 3 shows the values R_1 and R_2 for selected values of ϵ_i, $i = 1, 2, \ldots, 4$. Clearly, R_1 and R_2 decrease when ϵ_i are increased, and accordingly, the stability of EP_0 can be changed. Let us compute the critical value of the time delay that changes the stability of EP_0. Without loss of generality, we let the parameters $\epsilon_3 = \epsilon_4 = \epsilon_{34}$ and $\epsilon_1 = \epsilon_2 = \epsilon_{12}$, and write R_1 and R_2 as functions of ϵ_{34} and ϵ_{12}, respectively, as follows:

$$R_1(\epsilon_{34}) = \frac{\xi\mathfrak{J}\lambda e^{-(m_3+m_4)\epsilon_{34}}}{\beta\gamma\omega},$$
$$R_2(\epsilon_{12}) = \frac{a\gamma\eta\rho e^{-(m_1+m_2)\epsilon_{12}}}{\alpha\wp(\gamma k + \upsilon\xi)}. \tag{66}$$

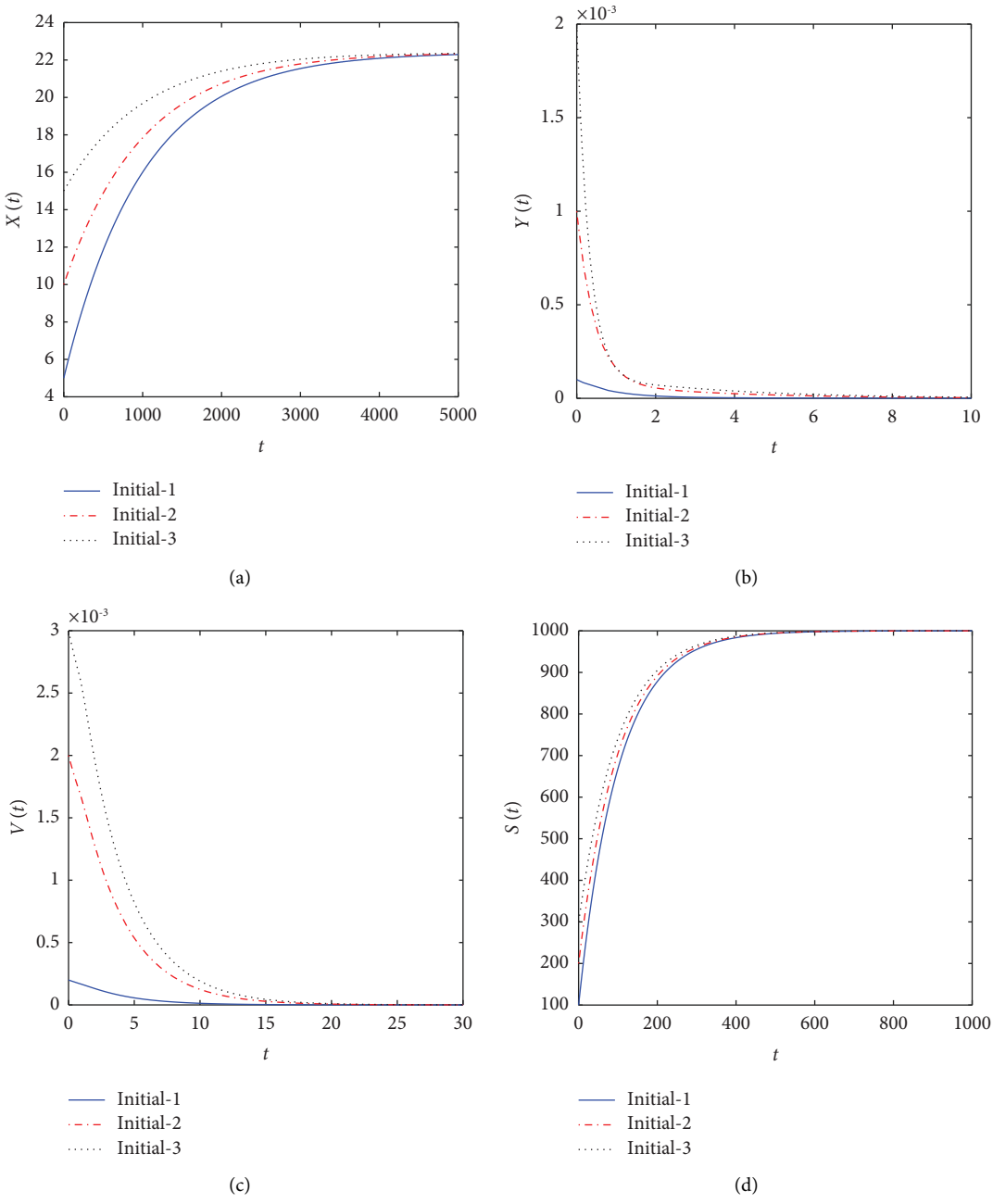

Figure 2: Continued.

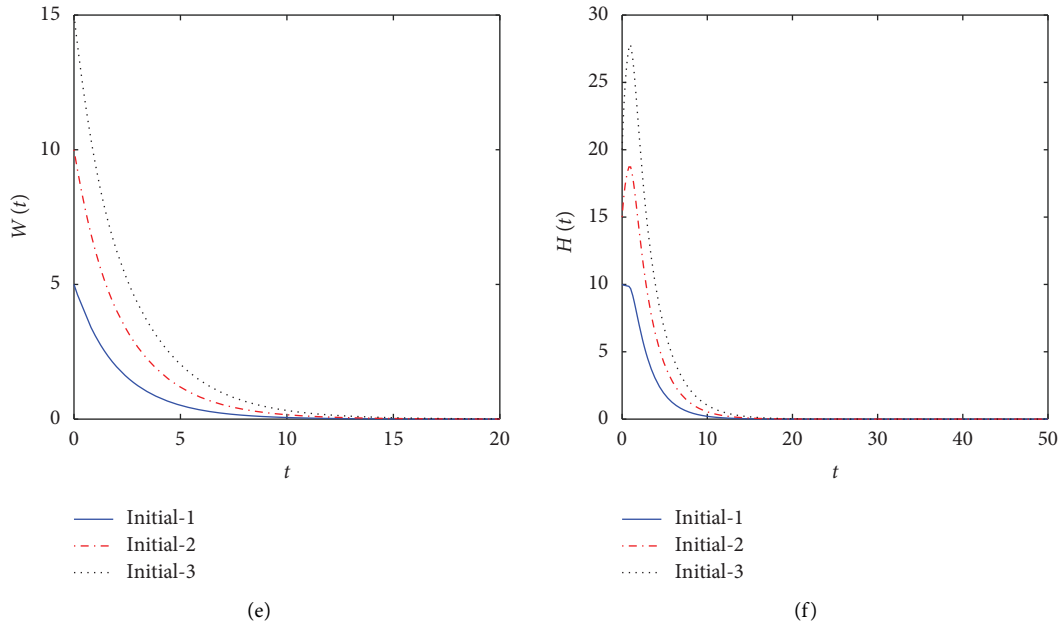

(e) (f)

FIGURE 2: The numerical simulations of model (64) for $\eta = 0.006$, $\upsilon = 0.01$, $\wp = 0.3$, and $\mathfrak{F} = 0.0001$ using three different initial conditions sets. Uninfected equilibrium $EP_0 = (22.41, 0, 0, 1000, 0, 0)$ is G.A.S. (a) Uninfected epithelial cells. (b) Infected epithelial cells. (c) SARS-CoV-2. (d) Uninfected $CD4^+$ T cells. (e) Infected $CD4^+$ T cells. (f) HIV-1.

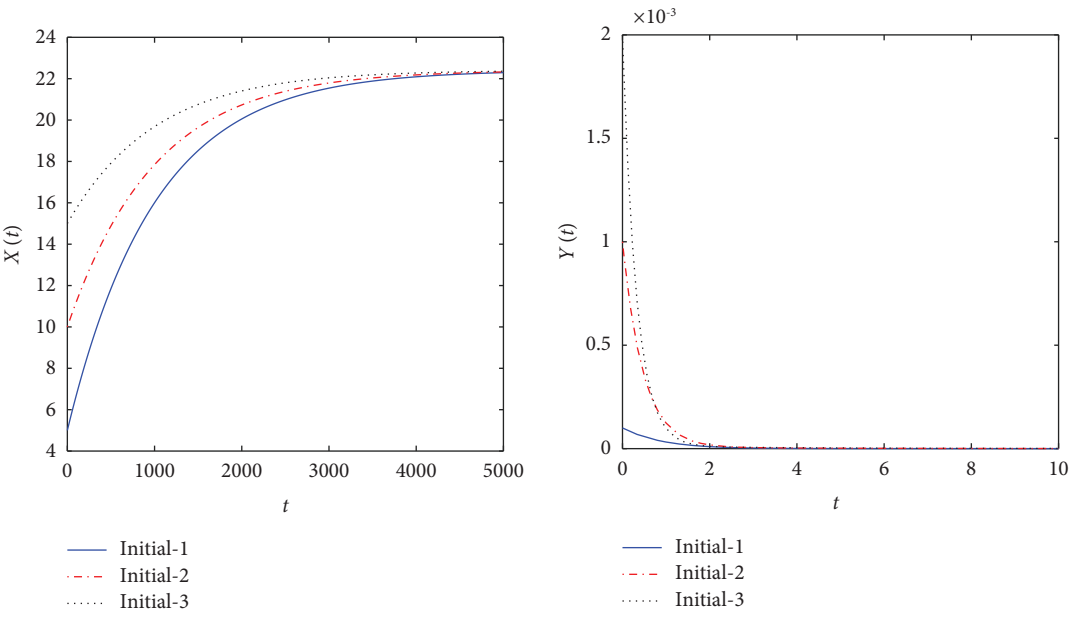

(a) (b)

FIGURE 3: Continued.

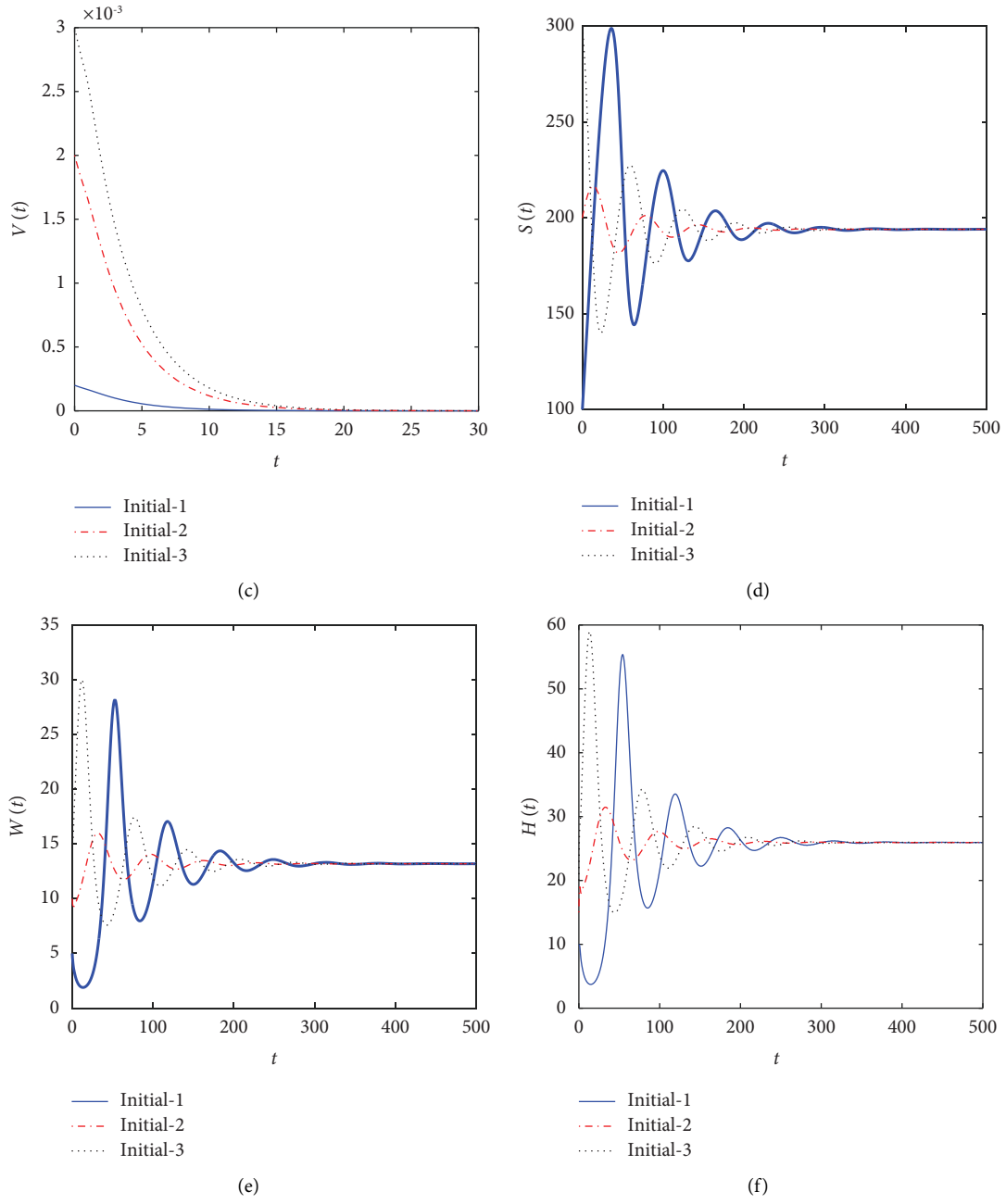

FIGURE 3: The numerical simulations of model (64) for $\eta = 0.0006$, $\upsilon = 0.01$, $\wp = 0.3$, and $\mathfrak{F} = 0.0016$ using three different initial conditions sets. HIV-1 monoinfection equilibrium $EP_H = (22.41, 0, 0, 186.478, 13.3211, 27.266)$ is G.A.S. (a) Uninfected epithelial cells. (b) Infected epithelial cells. (c) SARS-CoV-2. (d) Uninfected $CD4^+$ T cells. (e) Infected $CD4^+$ T cells. (f) HIV-1.

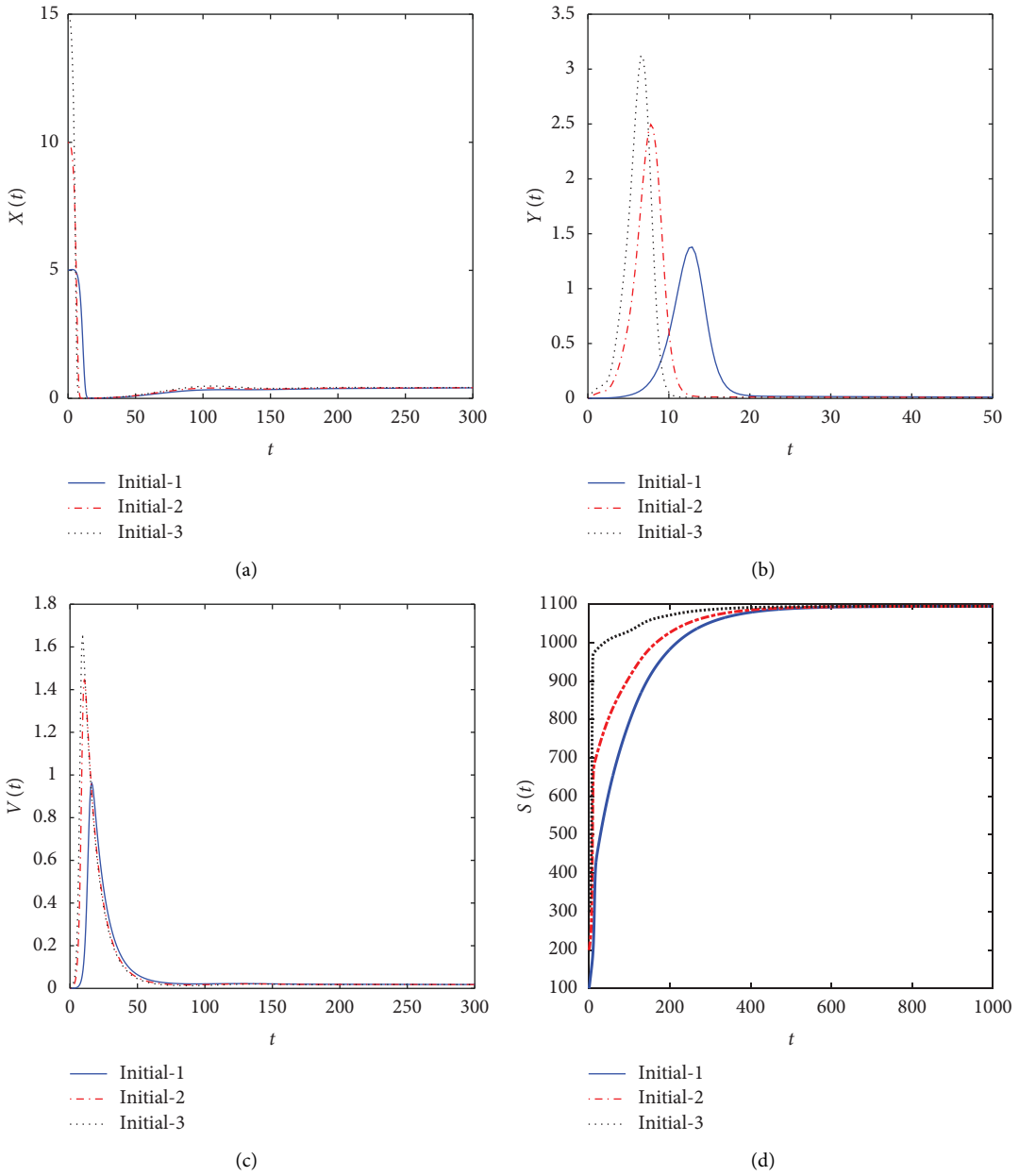

Figure 4: Continued.

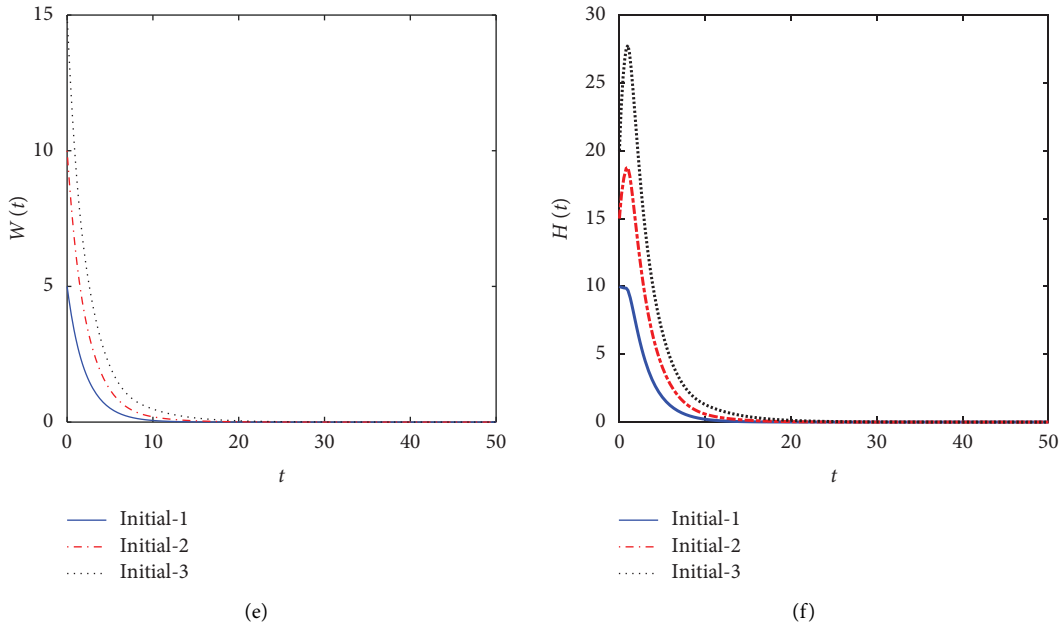

FIGURE 4: The numerical simulations of model (64) for $\eta = 2.9$, $\upsilon = 0.002$, $\wp = 0.1$, and $\mathfrak{F} = 0.0001$ using three different initial conditions sets. SARS-CoV-2 monoinfection equilibrium $EP_V = (0.4285, 0.0087, 0.018, 1094.69, 0, 0)$ is G.A.S. (a) Uninfected epithelial cells. (b) Infected epithelial cell. (c) SARS-CoV-2. (d) Uninfected $CD4^+$ T cells. (e) Infected $CD4^+$ T cells. (f) HIV-1.

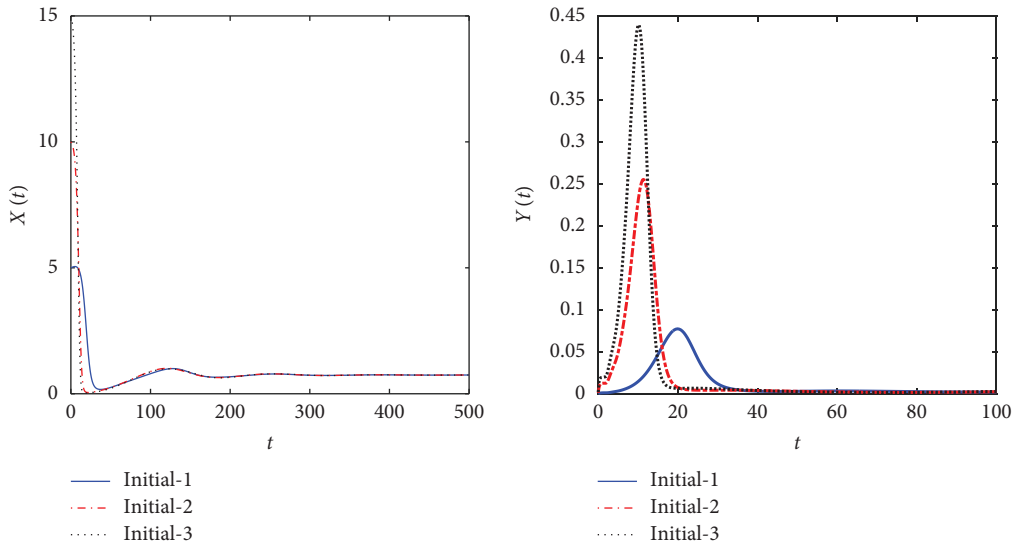

FIGURE 5: Continued.

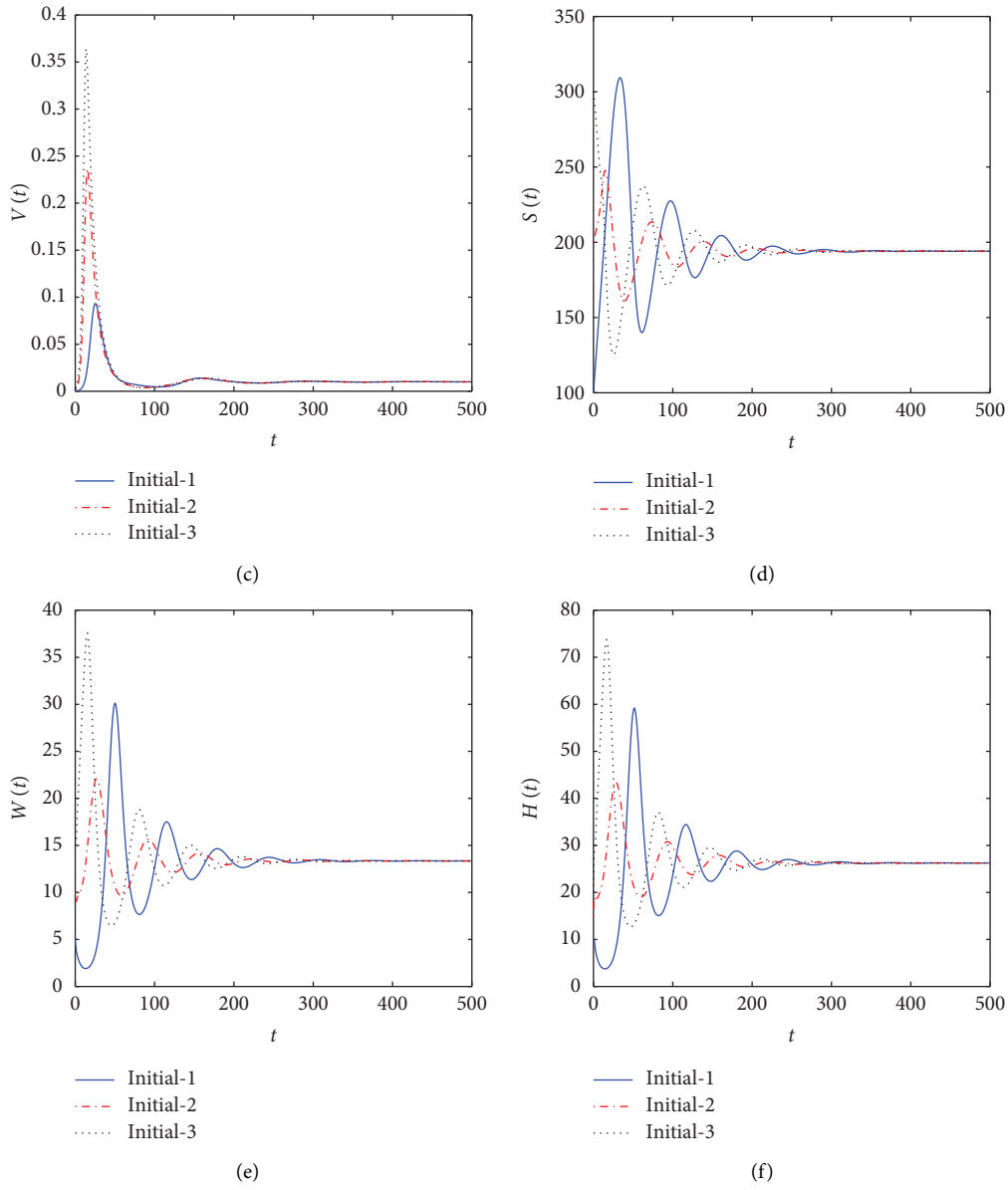

FIGURE 5: Model (64) numerical simulations for $\eta = 2.9$, $\upsilon = 0.02$, $\wp = 0.1$, and $\mathfrak{F} = 0.0016$ with three different initial conditions sets. COVID-19/AIDS coinfection equilibrium $EP_{VH} = (0.7155, 0.005, 0.0105, 186.478, 13.48, 27.59)$ is G.A.S. (a) Uninfected epithelial cells. (b) Infected epithelial cells. (c) SARS-CoV-2. (d) Uninfected $CD4^+$ T cells. (e) Infected $CD4^+$ T cells. (f) HIV-1.

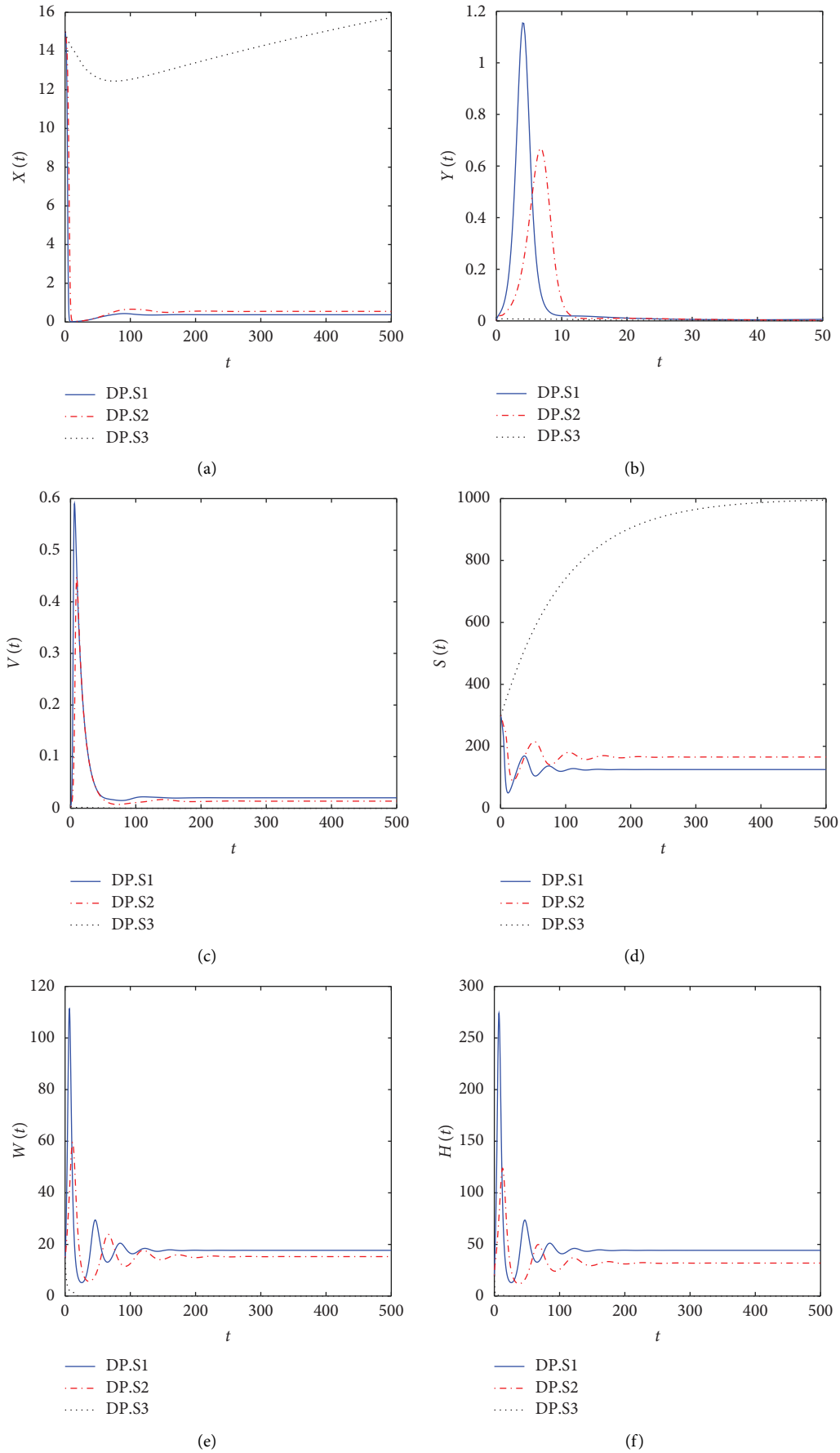

Figure 6: Model (64) numerical simulations for $\eta = 2.9$, $\upsilon = 0.02$, $\wp = 0.1$, and $\Im = 0.0016$ with three different sets of delay parameters. (a) Uninfected epithelial cells. (b) Infected epithelial cells. (c) SARS-CoV-2. (d) Uninfected $CD4^+$ T cells. (e) Infected $CD4^+$ T cells. (f) HIV-1.

Table 3: The variation of R_1 and R_2 with respect to the delay parameters.

Delay parameters	R_1	R_2
$\epsilon_{12} = \epsilon_{34} = 0$	8	7.75602
$\epsilon_{12} = 0.4$ and $\epsilon_{34} = 0.2$	7.24	6.88
$\epsilon_{12} = 0.6$ and $\epsilon_{34} = 0.4$	6.55	6.48
$\epsilon_{12} = 3$ and $\epsilon_{34} = 1$	4.85	3.15
$\epsilon_{12} = 5$ and $\epsilon_{34} = 3$	1.79	1.731
$\epsilon_{12} = 6.82823$ and $\epsilon_{34} = 4.15888$	1	1
$\epsilon_{12} = 7$ and $\epsilon_{34} = 5$	0.66	0.95
$\epsilon_{12} = 8$ and $\epsilon_{34} = 6$	0.3983	0.704
$\epsilon_{12} = 14$ and $\epsilon_{34} = 12$	0.0198	0.1163
$\epsilon_{12} = 18$ and $\epsilon_{34} = 16$	0.0027	0.035
$\epsilon_{12} = 24$ and $\epsilon_{34} = 20$	0.0004	0.0058

To compel basic reproduction numbers R_1 and R_2 to verify $R_1(\epsilon_{34}) \le 1$ and $R_2(\epsilon_{12}) \le 1$, respectively, we choose the following equations:

$$\epsilon_{34} \ge \epsilon_{34}^{\min}, \text{where } \epsilon_{34}^{\min} = \max\left\{0, \frac{1}{m_3 + m_4} \ln \frac{\xi \Im \lambda}{\beta \gamma \omega}\right\}. \quad (67)$$

And

$$\epsilon_{12} \ge \epsilon_{12}^{\min}, \text{where } \epsilon_{12}^{\min} = \max\left\{0, \frac{1}{m_1 + m_2} \ln \frac{a\gamma\eta\rho}{\alpha\wp(\gamma k + v\xi)}\right\}. \quad (68)$$

Therefore, if $\epsilon_{34} \ge \epsilon_{34}^{\min}$ and $\epsilon_{12} \ge \epsilon_{12}^{\min}$, then EP_0 is G.A.S. Computing ϵ_{34} and ϵ_{12} gives $\epsilon_{34} = 4.15888$ and $\epsilon_{12} = 6.82823$, respectively. It follows

(i) If $\epsilon_{34} \ge 4.15888$ and $\epsilon_{12} \ge 6.82823$, then $R_1(\epsilon_{34}) \le 1$, $R_2(\epsilon_{12}) \le 1$, and EP_0 is G.A.S.

(ii) If $\epsilon_{34} < 4.15888$ or $\epsilon_{12} < 6.82823$, then $R_1(\epsilon_{34}) > 1$, $R_2(\epsilon_{12}) > 1$, and EP_0 will lose its stability.

6. Discussion

Coinfection between COVID-19/AIDS has become a serious problem during COVID-19 pandemic. Mathematical modeling represents a main tool in helping experimental studies understand new diseases. We studied a within-host COVID-19/AIDS coinfection model with distributed delays in this paper. The model explores the contacts between healthy epithelial cells, infected epithelial cells, free SARS-CoV-2 particles, uninfected $CD4^+$ T cells, infected $CD4^+$ T cells, and free HIV-1 particles. There are four equilibrium points for the model with the following listed properties:

(a) Uninfected equilibrium EP_0: its existence is permanent and it is G.A.S if $R_1 \le 1$ and $R_2 \le 1$. This represents the situation of a person without SARS-CoV-2 or HIV-1 infections.

(b) The HIV-1 monoinfection equilibrium EP_H exists if $R_1 > 1$, and it is G.A.S if $R_4 \le 1$. At this point, the person has only HIV-1 infection, but he is not infected by SARS-CoV-2.

(c) SARS-CoV-2 monoinfection equilibrium EP_V is appeared when $R_2 > 1$, and if $R_3 \le 1$, then it is G.A.S. It is the instance of a person who is suffering from SARS-CoV-2 infection only.

(d) COVID-19/AIDS coinfection equilibrium EP_{VH} exists and G.A.S if $R_4 > 1$ and $1 < R_3 \le 1 + a\eta\Im\lambda\xi L_2 L_3 L_4/\beta\omega(u\alpha\wp + a\gamma\eta L_2)$. In this case, the patient suffers from COVID-19/AIDS coinfection.

The numerical and theoretical results were found to be in agreement. The time delays increase the concentrations of uninfected epithelial and $CD4^+$ T cells, while they decrease concentrations of free SARS-CoV-2 and HIV-1 particles. Thus, parameters of delay can be examined and used in developing effective treatments for COVID-19/AIDS coinfected patients. Moreover, the model with distributed delays confirmed the effect observed in [20] that low numbers of $CD4^+$ T cells can increase the risk of severe SARS-CoV-2 infection in coinfected patient. Thus, our model can be used to estimate the parameters required to get rid of SARS-CoV-2 in HIV-1 patients. Also, a bifurcation analysis can be executed in order to get a deeper understanding of the stability changes. Furthermore, the work can be developed by finding a better approximation of all parameters in model (2) through fitting with real data. We will keep these points in mind for future projects. [46].

Data Availability

No underlying data were collected or produced in this study.

Conflicts of Interest

The authors declare that they have no conflicts of interest.

Acknowledgments

The authors extend their appreciation to the Deanship of Scientific Research at King Khalid University, Abha, Saudi Arabia, for funding this work through the Research Group Project under grant number RGP.2/154/43.

References

[1] World Health Organization, *Coronavirus Disease (COVID-19), Weekly Epidemiological Update (27 April 2022)*World Health Organization (WHO), Geneva, Switzerland, 2022, https://www.who.int/publications/m/item/weekly-epidemiological-update-on-covid-19-27-april-2022.

[2] S. Richardson, J. S. Hirsch, M. Narasimhan et al., "Presenting characteristics, comorbidities, and outcomes among 5700 patients hospitalized with COVID-19 in the New York City Area," *JAMA*, vol. 323, pp. 2052–2059, 2020.

[3] F. E. Lithander, S. Neumann, E. Tenison et al., "COVID-19 in older people: a rapid clinical review," *Age and Ageing*, vol. 49, no. 4, pp. 501–515, 2020.

[4] S. Gatechompol, A. Avihingsanon, O. Putcharoen, K. Ruxrungtham, and D. R. Kuritzkes, "COVID-19 and HIV-1 infection co-pandemics and their impact: a review of the literature," *AIDS Research and Therapy*, vol. 18, no. 28, pp. 1–9, 2021.

[5] G. Unaids, *HIV-1 & AIDS Statistics-2018 Fact Sheet*, UNAIDS, Geneva, vol. 9, no. 1389 pages, 2021, http://www.unaids.org/en/resources/fact-sheet.

[6] R. Duerr, K. M. Crosse, A. M. Valero-Jimenez, and M. Dittmann, "SARS-CoV-2 portrayed against HIV: contrary viral strategies in similar disguise," *Microorganisms*, vol. 9, no. 1389, 61 pages, 2021.

[7] K. S. Sharov, "HIV/SARS-CoV-2 co-infection: T cell profile, cytokine dynamics and role of exhausted lymphocytes," *International Journal of Infectious Diseases*, vol. 102, no. 2021, pp. 163–169, 2021.

[8] T. Yoshikawa, T. Hill, K. Li, C. J. Peters, and C. T. K. Tseng, "Severe acute respiratory syndrome (SARS) coronavirus-induced lung epithelial cytokines exacerbate SARS pathogenesis by modulating intrinsic functions of monocyte-derived macrophages and dendritic cells," *Journal of Virology*, vol. 83, no. 7, pp. 3039–3048, 2009.

[9] J. D. Kowalska, A. Skrzat-Klapaczyńska, D. Bursa et al., "HIV care in times of the COVID-19 crisis - where are we now in Central and Eastern Europe," *International Journal of Infectious Diseases*, vol. 96, pp. 311–314, 2020.

[10] World Health Organization (Who), "Disruption in HIV, Hepatitis and STI Services Due to COVID-19," 2020, https://www.who.int/docs/default-source/hiv-hq/disruption-hiv-hepatitis-sti-services-due-to-covid19.pdf?sfvrsn=5f78b742_6.

[11] P. K. Drain and N. Garrett, "SARS-CoV-2 pandemic expanding in sub-Saharan Africa: considerations for COVID-19 in people living with HIV," *EClinicalMedicine*, vol. 22, Article ID 100342, 2 pages, 2020.

[12] C. Yang, Y. Yang, Z. Li, and L. Zhang, "Modeling and analysis of COVID-19 based on a time delay dynamic model," *Mathematical Biosciences and Engineering*, vol. 18, no. 1, pp. 154–165, 2021.

[13] C. Pinnetti, A. Vergori, C. Agrati et al., "SARS-CoV-2 infection does not induce HIV viral escape in the central nervous system: a case series," *International Journal of Infectious Diseases*, vol. 101, pp. 38–41, 2020.

[14] F. Schmidt, Y. Weisblum, F. Muecksch et al., "Measuring SARS-CoV-2 neutralizing antibody activity using pseudotyped and chimeric viruses," *Journal of Experimental Medicine*, vol. 217, no. 11, Article ID e20201218, 2020.

[15] V. K. Shah, P. Firmal, A. Alam, D. Ganguly, and S. Chattopadhyay, "Overview of immune response during SARS-CoV-2 infection: lessons from the past," *Frontiers in Immunology*, vol. 11, no. 1949, 17 pages, 2020.

[16] M. Wang, L. Luo, H. Bu, and H. Xia, "One case of coronavirus disease 2019 (COVID-19) in a patient co-infected by HIV with a low CD4+ T-cell count," *International Journal of Infectious Diseases*, vol. 96, pp. 148–150, 2020.

[17] M. Wu, F. Ming, S. Wu et al., "Risk of SARS-CoV-2 infection among people living with HIV in wuhan, China," *Frontiers in Public Health*, vol. 10, Article ID 833783, 2022.

[18] A. M. Elaiw, "Global properties of a class of HIV models," *Nonlinear Analysis: Real World Applications*, vol. 11, no. 4, pp. 2253–2263, 2010.

[19] A. S. Perelson, D. E. Kirschner, and R. De Boer, "Dynamics of HIV infection of CD4+ T cells," *Mathematical Biosciences*, vol. 114, no. 1, pp. 81–125, 1993.

[20] A. D. Al Agha, A. M. Elaiw, S. A. Azoz, and E. Ramadan, "Stability analysis of within-host SARS-CoV-2/HIV coinfection model," *Mathematical Methods in the Applied Sciences*, vol. 45, no. 17, pp. 1–20, 2022.

[21] A. M. Elaiw, A. D. Al Agha, S. A. Azoz, and E. Ramadan, "Global analysis of within-host SARS-CoV-2/HIV coinfection model with latency," *The European Physical Journal Plus*, vol. 137, no. 2, pp. 174–222, 2022.

[22] N. Ringa, M. L. Diagne, H. Rwezaura, A. Omame, S. Y. Tchoumi, and J. M. Tchuenche, "HIV and COVID-19 co-infection: a mathematical model and optimal control," *Informatics in Medicine Unlocked*, vol. 31, Article ID 100978, 2022.

[23] M. A. Zaitri, C. J. Silva, and D. F. M. Torres, "Stability analysis of delayed COVID-19 models," *Axioms*, vol. 11, no. 8, pp. 400–421, 2022.

[24] B. J. Nath, K. Dehingia, V. N. Mishra, Y. M. Chu, and H. K. Sarmah, "Mathematical analysis of a within-host model of SARS-CoV-2," *Advances in Difference Equations*, vol. 2021, no. 113, pp. 1–11, 2021.

[25] A. S. Perelson, P. Essunger, Y. Cao et al., "Decay characteristics of HIV-1-infected compartments during combination therapy," *Nature*, vol. 387, no. 6629, pp. 188–191, 1997.

[26] Y. Li, R. Xu, Z. Li, and S. Mao, "Global dynamics of a delayed HIV-1 infection model with CTL immune response," *Discrete Dynamics in Nature and Society*, vol. 2011, Article ID 673843, 13 pages, 2011.

[27] A. D. AlAgha and A. M. Elaiw, "Stability of a general reaction-diffusion HIV-1 dynamics model with humoral immunity," *The European Physical Journal Plus*, vol. 134, no. 8, pp. 390–418, 2019.

[28] R. V. Culshaw and S. Ruan, "A delay-differential equation model of HIV infection of $CD4^+$ T-cells," *Mathematical Biosciences*, vol. 165, no. 1, pp. 27–39, 2000.

[29] A. M. Elaiw and A. D. Al Agha, "Global dynamics of SARS-CoV-2/cancer model with immune responses," *Applied Mathematics and Computation*, vol. 408, no. 126364, 20 pages, 2021.

[30] C. Li, J. Xu, J. Liu, and Y. Zhou, "The within-host viral kinetics of SARS-CoV-2," *Mathematical Biosciences and Engineering*, vol. 17, no. 4, pp. 2853–2861, 2020.

[31] S. Q. Du and W. Yuan, "Mathematical modeling of interaction between innate and adaptive immune responses in COVID-19 and implications for viral pathogenesis," *Journal of Medical Virology*, vol. 92, no. 9, pp. 1615–1628, 2020.

[32] A. E. S. Almocera, G. Quiroz, and E. A. Hernandez-Vargas, "Stability analysis in COVID-19 within-host model with immune response," *Communications in Nonlinear Science and Numerical Simulation*, vol. 95, Article ID 105584, 2021.

[33] L. Pinky and H. M. Dobrovolny, "SARS-CoV-2 coinfections: could influenza and the common cold be beneficial," *Journal of Medical Virology*, vol. 92, pp. 1–8, 2020.
[34] I. Ahmed, E. F. Doungmo Goufo, A. Yusuf, P. Kumam, P. Chaipanya, and K. Nonlaopon, "An epidemic prediction from analysis of a combined HIV/COVID-19 co-infection model via ABC-fractional operator," *Alexandria Engineering Journal*, vol. 60, no. 3, pp. 2979–2995, 2021.
[35] D. Adak and N. Bairagi, "Analysis and computation of multi-pathways and multi-delays HIV-1 infection model," *Applied Mathematical Modelling*, vol. 54, pp. 517–536, 2018.
[36] F. V. Atkinson and J. R. Haddock, "On determining phase spaces for functional differential equations," *Funkcialaj Ekvacioj*, vol. 31, pp. 331–347, 1988.
[37] J. K. Hale and S. M. V. Lunel, *Introduction to functional differential equations*, Science & Business Media, Springer, 2013.
[38] Y. Kuang, *Delay Differential Equations with Applications in Population Dynamics*, Academic Press, Cambridge, MA, USA, vol. 191, pp. 3–12, 1993.
[39] A. Korobeinikov, "Global properties of basic virus dynamics models," *Bulletin of Mathematical Biology*, vol. 66, no. 4, pp. 879–883, 2004.
[40] E. A. Barbashin, *Introduction to the Theory of Stability*, Wolters-Noordhoff, Groningen, Netherlands, 1970.
[41] J. P. La Salle, *The Stability of Dynamical Systems*, Society for Industrial and Applied Mathematics, Philadelphia, 1976.
[42] A. M. Lyapunov, "The general problem of the stability of motion," *International Journal of Control*, vol. 55, no. 3, pp. 531–534, 1992.
[43] A. S. Perelson and P. W. Nelson, "Mathematical analysis of HIV-1 dynamics in vivo," *SIAM Review*, vol. 41, no. 1, pp. 3–44, 1999.
[44] M. Prakash, R. Rakkiyappan, A. Manivannan, and J. Cao, "Dynamical analysis of antigen-driven T-cell infection model with multiple delays," *Applied Mathematics and Computation*, vol. 354, pp. 266–281, 2019.
[45] D. S. Callaway and A. S. Perelson, "HIV-1 infection and low steady state viral loads," *Bulletin of Mathematical Biology*, vol. 64, no. 1, pp. 29–64, 2002.
[46] Y. Yang and A. Iwasaki, "Impact of chronic HIV infection on SARS-CoV-2 infection, COVID-19 disease and vaccines," *Current HIV*, vol. 19, no. 1, pp. 5–16, 2021.